UNIVERSITÀ
DEGLI STUDI
DI PADOVA

Novel Results on Slow Coherency in Power Networks

M.S. candidate: Diego Romeres

Advisor: Prof. Ruggero Carli
Prof. Sandro Zampieri
Prof. Luca Schenato
Co-Advisor: Prof. Francesco Bullo
PhD. Florian Dörfler

M.S. School in Automation Engineering

Department of Information Engineering

2011

Summary

The thesis was conducted during a period of six months at the University of California of Santa Barbara in collaboration with Prof. F. Bullo and the PhD student Florian Dörfler. An article was submitted for the European Control Conference 2013-Zurig.

In this thesis we revisit the classic slow coherency and area aggregation approach to model reduction in power networks. The slow coherency approach is based on identifying sparsely and densely connected areas of a network, within which all generators swing coherently. A time-scale separation and singular perturbation analysis then results in a reduced low-order system, where coherent areas are collapsed into aggregate variables.

Here, we study the application of slow coherency and area aggregation to first-order consensus systems and second-order power system swing dynamics. We unify different theoretic approaches and ideas found throughout the literature, we relax some technical assumptions, and we extend existing results. In particular, we provide a complete analysis of the second-order swing dynamics – without restrictive assumptions on the system damping.

Contents

1
Introduction

A power network is a large-scale and complex dynamical system. Here the attribute "complex" refers to both rich dynamics of the individual system component as well as their non-trivial interaction through the network. In order to tackle this complexity for analysis, control design, and monitoring schemes, it is of interest to construct reduced-order models which preserve the dynamics of interest.

In this work, we are interested in electromechanical *inter-area dynamics*, which are associated with the dynamics of power transfers and involve groups of generators oscillating relative to each other. In a heavily stressed grid, poorly damped inter-area oscillations can even become unstable, as seen in the blackout of August 10, 1996 in the Western American network Venkatasubramanian and Li (2004).

To achieve a better understanding of the complex inter-area dynamics of a large-scale power grid, a natural approach is to collapse groups of coherent machines into single equivalent machines and study the dynamics of such a reduced model. Intuitively, these coherent groups can be identified as strongly connected components of the weighted graph, and entire geographic areas of a power grid can be aggregated to single equivalent models.

The approach outlined above has been refined in the pioneering work on *slow coherency* by Chow et al., see the seminal papers Chow (1982); Chow and Kokotović

(1985); Chow, Cullum, and Willoughby (1984); Date and Chow (1991); Chow, Allemong, and Kokotović (1978) among others. Slow coherency theory considers power network models, such as the RTS 96 in Figure 5.1, that are naturally partitioned into areas, which are internally densely connected and weakly connected to each other. Next, aggregate variables are defined for each area corresponding to the area's center of mass (or inertia). These aggregate variables describe the collective area dynamics, and they are complemented by a set of local variables representing the incoherency within the areas. A singular perturbation analysis shows that the long-term inter-area dynamics are determined by the aggregate variables.

The reduced-order model is the system resulting from the singular perturbation analyzis composed only by the aggregate variables. There are several advantages of reducing the order of the model

- Model Identification: the real network can have an intractable number of nodes, therefore a chaotic formulation;

- Simpler and efficient protocols can be used for routing and broadcasting within an aggregate area;

- Data storage requirement is modest;

- Less computation;

- Less states in the system to control.

A recent application of slow coherency theory is measurement-based identification of the aggregate models for monitoring and control purposes Chakrabortty, Chow, and Salazar (2011).

Consider for example the Western Systems Coordinating Council (WSCC) represented in figure fig: PowerNetworkWSCC, thus roughly represent the power network of the west coast of the United States.

The black dots are a pure illustrative approximations of the generators existing. In such a network there can be thousands or even millions of nodes and it is clear how hard it would be to study the associated model. Whereas, a model composed by 9 states, one for each area, approximating the original one would render the analyzis feasible. It is on this reasoning that this project is based.
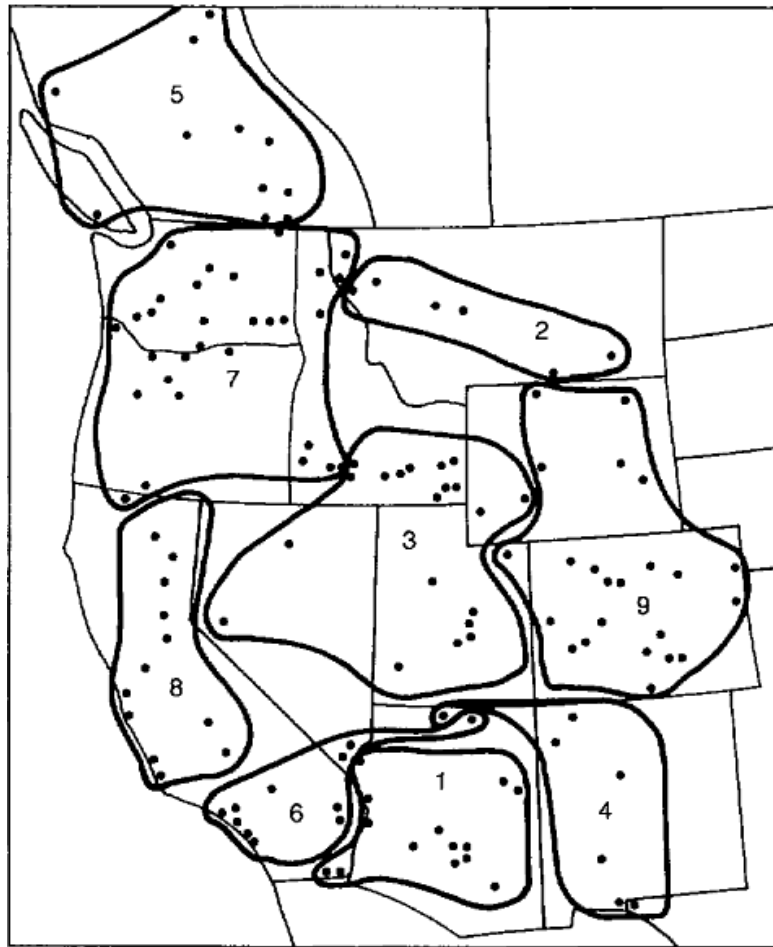
Figure 1.1: 9-Areas partitioning of the Western Systems Coordinating Council.

Literature review. The problem of aggregation and slow coherency has attracted tremendous scientific interest in networked control and power systems.

In Chow (1982) and Chow and Kokotović (1985) the foundations of area aggregation are laid out for first and second-order linear interconnected systems with diffusive coupling. The authors determined a rigorous method to trace the dynamic of a large power network into an explicit singular perturbation form system. Moreover, they started the analysis of the resulting aggregate system, which is the object of interest in our work.

These networked systems correspond to either consensus dynamics Bullo, Cortés, and Martínez (2009); Garin and Schenato (2010) or the electromechanical swing dynamics of network-reduced power systems Sauer and Pai (1998); Dörfler

and Bullo (2011).

Recently, the methods developed in Chow (1982); Chow and Kokotović (1985) have been extended to non-linearly coupled first-order systems Bıyık and Arcak (2007).

The second-order case has been heavily investigated in the context of power systems Chow et al. (1984); Date and Chow (1991); Chow and Kokotović (1985); Chow et al. (1978); Chow (1982). In Chow et al. (1984) a sparsity-based technique is developed to identify coherent areas, and in Date and Chow (1991) the singular perturbation and aggregation presented in Chow and Kokotović (1985) has been further refined. The articles Chow and Kokotović (1985); Date and Chow (1991); Chow et al. (1984) do not take the system damping into account, which is a technically inconvenient obstacle in the aggregation analysis.

In Chow et al. (1978), a singular perturbation analysis of a second-order dissipative system was carried out, but the resulting slow and fast systems are required to have high frequency oscillations. Thus, some strong structural conditions on the initial system have to be met.

The recent Mallada and Tang (2011) deals with second order systems with damping and it points out the relations between damping, power scheduling and line impedances. The damping of the system is also related to some characteristics of the Laplacian matrix and its fundamental for the stability of the system, these reasons contributed to our interest in the analyzis of general second order systems.

Finally, in Chow (1982) an approach to second-order dissipative systems is presented, which is based on a restrictive uniform damping assumption and on an incomplete analysis.

Contribution   In this paper, we review the different existing approaches Chow (1982); Chow and Kokotović (1985); Chow et al. (1984); Date and Chow (1991); Chow et al. (1978); Bıyık and Arcak (2007) to slow coherency in a unified language.

We analyze the two cases of first-order consensus dynamics and second-order swing dynamics in power networks. We combine and extend the existing analysis approaches, and we remove some technical assumptions commonly made in the literature, such as regularity assumptions and assumptions on the graph connectivity. We also formally extend the existing theory to weighted graphs.

More importantly, we provide a complete and detailed analysis of area aggregation for the second-order case with damping. The resulting aggregate model equals the one proposed in Chow (1982); Chow et al. (1978), but we do not assume restrictive structural constraints or uniform damping.

Finally, motivated by remarks in Chow and Kokotović (1985), we identify the reduced aggregate models as generalized consensus systems Bullo et al. (2009); Olfati-Saber, Fax, and Murray (2007) with multiple time constants (in the first-order case), aggregate damping and inertia matrices (in the second-order case), and possibly adverse interactions among the aggregate nodes (corresponding to negative coupling weights).

We illustrate our developments with simulations of the RTS 96 system and of random densely connected graphs generated with routines based on Erdös-RÃľnyi algorithm.

Thesis organization Chapter 2 presents the problem setup and summarizes the area aggregation process for consensus systems. In particular, we define mathematically the concept of sparsely connected area and we perform the singular perturbation analyzis together with the description of the multi time-scale separation, which is one of its major properties.

Chapter 3 identifies the aggregate model as a generalized Laplacian system and states the convergence to the same consensus point of the original and of the reduced order system.

Chapter 4 extends the results from the first-order consensus dynamics to the second-order swing equations. The analyzis followed is the same also for the second order dynamic, therefore in this chapter, all the mathematical issues which appear passing through this more complicated system are demonstrated and explained.

Chapter 5 illustrates our theoretical results with simulation studies. The simulations test both an official power network the RTS96 which is naturally created with the structure of sparse connected areas and with several random networks that we implemented.

Finally, chapter 6 concludes the thesis describing the major results obtained.

The remainder of this chapter recalls some preliminaries and introduces some notation.

Preliminaries and notation

Vectors and matrices: Let $\mathbf{1}_n$ and $\mathbf{0}_n$ be the n-dimensional vectors of unit and zero entries, respectively. Let $I_n \in \mathbb{R}^{n \times n}$ be the n-dimensional identity matrix.

For a symmetric matrix $A = A^T \in \mathbb{R}^{n \times n}$ we write $A > 0$, $A \succeq 0$, $A < 0$, and $A \preceq 0$ if A is positive definite, positive semidefinite, negative definite, negative semidefinite, respectively.

Given an array $\{x_i\}_{i \in 1,\ldots,n}$, let $x \in \mathbb{R}^n$ be the associated vector, and let $\text{diag}(x) \in \mathbb{R}^{n \times n}$ be the associated diagonal matrix.

Sets: Given a discrete set $\mathcal{X}$, denote its cardinality by $|\mathcal{X}|$.

Algebraic graph theory: Consider a connected, undirected, and weighted graph $G = (\mathcal{V}, \mathcal{E}, W)$, where $\mathcal{V} = 1,\ldots,n$ is the set of nodes, $\mathcal{E} \subset \mathcal{V} \times \mathcal{V}$ is the set of undirected edges, and $W = W^T \in \mathbb{R}^{n \times n}$ is the adjacency matrix with entries $w_{ij} > 0$ if $\{i,j\} \in \mathcal{E}$ and $w_{ij} = 0$ otherwise.

What is the physical meaning of the weights on the edges is not really the point of our work, but the reader can think to them as electrical impedances, since we are working with power networks.

An electrical impedances is the complex ratio of the voltage over the current in an alternating current (AC) circuit and it is formed by a real part, the resistance, and an imaginary part the reactance.

$$Z = |Z|e^{j\theta}, \quad \text{with } |Z| = |R + iX|.$$

where R is the resistance, X is the reactance and θ is the phase between the two.

Throughout the paper, we implicitly assume that all nonzero edge weights are uniformly non-degenerate and bounded, that is, there are $\underline{w}, \overline{w} \in \mathbb{R}$ such that

$$0 < \underline{w} \leq w_{ij} \leq \overline{w}, \quad \forall \{i,j\} \in \mathcal{E}.$$

The following graph matrices and their properties will be of interest to us Biggs (1994). The degree matrix $D \in \mathbb{R}^{n \times n}$ is the diagonal matrix with elements $d_{ii} = \sum_{j=1, j \neq i}^{n} w_{ij}$. The Laplacian matrix $L = L^T \in \mathbb{R}^{n \times n}$ is defined by $L = D - W$, and it satisfies $L \succeq 0$ and $L\mathbf{1}_n = \mathbf{0}_n$. Defined component-wise the weighted Laplacian

matrix is:

$$l_{i,j} \triangleq \begin{cases} -w(i,j) & \text{if } i \neq j \text{ and } \{i,j\} \in \mathcal{E} \\ |\sum_{j=1}^{n} w(i,j)| & \text{if } i = j \\ 0 & \text{otherwise} \end{cases}$$

If a number $\ell \in 1,\dots,|\mathcal{E}|$ and an arbitrary direction is assigned to each edge $\{i,j\} \in \mathcal{E}$, the (oriented) *incidence matrix* $B \in \mathbb{R}^{n \times |\mathcal{E}|}$ is defined component-wise by

$$B_{k\ell} \triangleq \begin{cases} 1 & \text{if node } k \text{ is the sink node of edge } \ell \\ -1 & \text{if node } k \text{ is the source node of edge } \ell \\ 0 & \text{otherwise} \end{cases}$$

For $x \in \mathbb{R}^n$, the vector $B^T x$ has components $x_i - x_j$ corresponding to the oriented edge from j to i.

If $\text{diag}(\{w_{ij}\}_{\{i,j\}\in\mathcal{E}})$ is the diagonal matrix of edge weights, then $L = B \, \text{diag}(\{w_{ij}\}_{\{i,j\}\in\mathcal{E}}) B^T$.

If the graph is connected, then $\text{Ker}(B^T) = \text{Ker}(L) = \text{span}(\mathbf{1}_n)$ and all $n-1$ non-zero eigenvalues of L are strictly positive.

2

Aggregation and Slow Coherency

In this chapter, we introduce the problem setup in slow coherency analysis and present a brief yet complete analyzis of time-scale separation and area aggregation.

In the problem setup we mainly characterize the dynamics of the network. The other sections illustrate the procedure to transform these dynamics into the standard singular perturbation form which yields the aggregate system.

2.1 Mathematical models and problem setup

Consider a connected, undirected, and weighted graph $G = (\mathcal{V}, \mathcal{E}, W)$ with n nodes, Laplacian matrix L, and incidence matrix B.

Associated to this graph, we consider two different dynamical systems. The first system is the widely adapted *consensus protocol* Bıyık and Arcak (2007); Chow and Kokotović (1985); Olfati-Saber et al. (2007). Considers n autonomous agents. Each agent $i \in 1, \ldots, n$ is equipped with a local state variable x_i, and the agents exchange their states according to the first-order *consensus dynamics*

$$\dot{x} = -Lx.\tag{2.1}$$

A spectral analysis Olfati-Saber et al. (2007) of the consensus dynamics (2.1) reveals that asymptotically all agents synchronize to a common consensus state, that is, $\lim_{t\to\infty} x_i(t) = \lim_{t\to\infty} x_j(t) = x_\infty \in \mathbb{R}$ for all $i, j \in 1, \ldots, n$. In particular, the asymptotic consensus state is given by $x_\infty = \sum_{i=1}^n x_i(0)/n$.

A natural extension of the first-order consensus protocol (2.1) to a second-order mechanical system can be achieved as follows. With each node $i \in 1, \ldots, n$, we associate an inertia coefficient $M_i > 0$ and a damping coefficient $D_i > 0$. Let $M \in \mathbb{R}^{n \times n}$ and $D \in \mathbb{R}^{n \times n}$ be the diagonal matrices of inertia and damping coefficients, and consider the second-order dissipative consensus dynamics

$$M\ddot{x} = -D\dot{x} - Lx. \tag{2.2}$$

Our enabling application of interest for the second-order consensus dynamics (2.2) is given by the electromechanical swing dynamics of large-scale electric power networks Sauer and Pai (1998); Chow (1982); Chow and Kokotović (1985); Date and Chow (1991); Chow et al. (1978, 1984). Here each node $i \in 1, \ldots, n$ corresponds to a synchronous generator or a load (modeled as a synchronous motor) with inertia M_i damping D_i, and rotor angle x_i, and L is the incremental admittance matrix, arising from a Jacobian linearization and Kron reduction Dörfler and Bullo (2011) of the nonlinear power network dynamics. For the remainder of the paper, we refer to system (2.2) simply as *power network dynamics*.

In the following, we will assume that the graph G is partitioned in r areas, that is, $\mathcal{V} = \bigcup_{\alpha=1}^r \mathcal{V}_\alpha$ with $\mathcal{V}_\alpha$ being the node set of area α. We denote the number of nodes in area α by $m_\alpha = |\mathcal{V}_\alpha|$.

The edge set of area α is given by $\mathcal{E}_\alpha = \mathcal{E} \cap \{\mathcal{V}_\alpha \times \mathcal{V}_\alpha\}$.

We assume that the partition is such that each subgraph $(\mathcal{V}_\alpha, \mathcal{E}_\alpha)$ is connected for $\alpha \in 1, \ldots, r$.

Finally, we define the internal set edge $\mathcal{E}_{\text{int}}$ by $\mathcal{E}_{\text{int}} = \bigcup_{\alpha=1}^r \mathcal{E}_\alpha$ and the external edge set $\mathcal{E}_{\text{ext}}$ by $\mathcal{E}_{\text{ext}} = \mathcal{E} \setminus \mathcal{E}_{\text{int}}$. Notice that $\mathcal{E} = \mathcal{E}_{\text{int}} \cup \mathcal{E}_{\text{ext}}$.

Accordingly, define the external adjacency matrix $W^E \in \mathbb{R}^{n \times n}$ with elements $w_{ij}^E = w_{ij}$ if $\{i, j\} \in \mathcal{E}_{\text{ext}}$ and the internal adjacency matrix by $W^I = W - W^E \in \mathbb{R}^{n \times n}$.

The associated degree matrices are $D^E \in \mathbb{R}^{n \times n}$ with $d_{ii}^E = \sum_{j=1, j\neq i}^n w_{ij}^E$ and $D^I \in \mathbb{R}^{n \times n}$ with elements $d_{ii}^I = \sum_{j=1, j\neq i}^n w_{ij}^I$.

Finally, define the *internal Laplacian* $L^I = D^I - W^I \in \mathbb{R}^{n \times n}$ and the *external*

Laplacian $L^E = D^E - W^E \in \mathbb{R}^{n \times n}$. By construction, we obtain

$$L = L^I + L^E. \tag{2.3}$$

Accordingly, define B^I and B^E as the incidence matrices B associated to $L^I = B^I \operatorname{diag}(\{w_{ij}\}_{\{i,j\} \in \mathcal{E}_{\text{int}}})B_I$ and $L^E = B^E \operatorname{diag}(\{w_{ij}\}_{\{i,j\} \in \mathcal{E}_{\text{ext}}})B_E$, respectively.

In the following, we will be particularly interested in the case, where each of the r areas is internally densely connected, and distinct areas are sparsely connected among another.

Given such a partition of the graph, it is reasonably to expect that nodes within each area strongly interact with each other and quickly synchronize their states $x_i(t)$ according to the inner-area dynamics induced by L^I. On the other hand, we also expect that nodes from disjoint areas interact only weakly, and the long-term behavior of (2.1) and (2.2) will depend mostly on inter-area dynamics induced by L^E rather than inner-area dynamics.

In the following sections we make this intuition precise and formalize the particular notions of dense and sparse connections, time-scale separation, as well as inter-area and inner-area dynamics.

Example

Throughout this Chapter we consider a simple example graph, partitioned with sparse and densely connected areas, with the intention of illustrating the theoretical results we are going to achieve and help the reader in better understanding them.

Considering the graph in Figure 2.1 and implementing it in Matlab with random initial conditions, the nodes obey to dynamics (2.1) and their evolution on time looks like Figure 2.2.

Figures 2.1 and 2.2 show the reasoning behind determining an aggregate model. All the coloured lines represent the dynamic of one single node until they collapse, in a single line, which represents the dynamic of one area. In this example all the nodes within an area reach the same value in a short time, which can be considered negligible respect to the time needed for the all system to reach the global consensus. This is why an aggregate model of 3 states instead of 13 seems
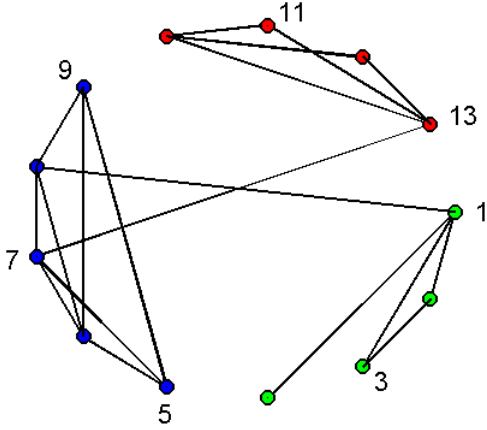
Figure 2.1: 3-Areas and 13-nodes graph.
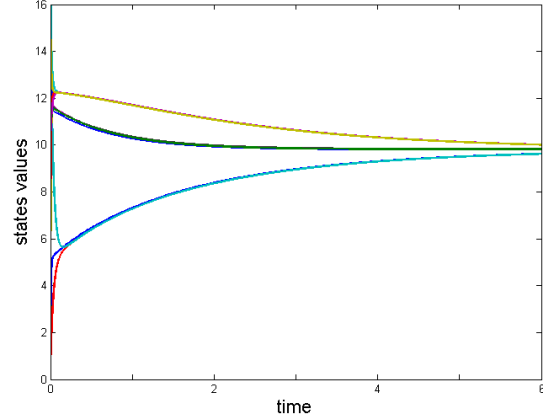
Figure 2.2: Evolution of the graph with first order dynamics

reasonable for this graph.

In addition, notice that the area composed by nodes 1 to 4 (the green ones) in Figure 2.1 is less internally connected compared to the other two areas. This corresponds to the dynamic of the nodes which aggregate in the lowest group of Figure 2.2. The time needed by these nodes to aggregate is longer than in the other areas, this result coincides with the common results in consensus problems where the agents achieve consensus faster accordingly with an increasing coupling between them.

2.2   Characterization of connectivity and sparsity

We quantify the trade-off of internally densely connected and externally sparsely connected areas by two numerical parameters: a node parameter and an area parameter.

Node parameter   For each area $\alpha \in 1,\dots,r$ and each node $i \in \mathcal{V}_\alpha$, define the *internal degree* $c^I_{\alpha,i}$ and the *external degree* $c^E_{\alpha,i}$ by

$$c^I_{\alpha,i} = \sum_{\{i,j\}\in\mathcal{E}_\alpha} w_{ij} \quad \text{and} \quad c^E_{\alpha,i} = \sum_{\{i,j\}\in\mathcal{E}_{\text{ext}}} w_{ij}.$$

those in words are:

$c_{\alpha i}^I$ = the sum of the weighted internal connections of node i in area α,

$c_{\alpha i}^E$ = the sum of the weighted external connections of node i in area α.

The *node parameter d* is then given by the worst-case ratio of the internal and external degree over all nodes and areas:

$$d = \frac{\max_{\alpha \in 1,\dots,r, i \in \mathcal{V}_\alpha} c_{\alpha,i}^E}{\min_{\alpha \in 1,\dots,r, i \in \mathcal{V}_\alpha} c_{\alpha,i}^I} = \frac{c^E}{c^I}. \tag{2.4}$$

If condition $d \ll 1$ holds, it means that each node has stronger connections with the other nodes within its own area than the connections with the other nodes belonging to different areas.

Area Parameter   For each area $\alpha \in 1,\dots,r$, define the *internal edge weight γ_α^I* and the *external edge weight γ_α^E* by

$$\gamma_\alpha^I = \sum_{\{i,j\} \in \mathcal{E}_\alpha} w_{ij} \quad \text{and} \quad \gamma_\alpha^E = \sum_{\{i,j\} \in \mathcal{E}_{\text{ext}}} w_{ij}.$$

those in words are:

γ_α^I = the total sum of the weighted internal connections over all nodes within area α,

γ_α^E = the total sum of the weighted external connections over all nodes within area α.

Analogously to the node parameter, we aim to define an area parameter by the worst-case ratio of the internal and external edge weight. Notice that $\gamma_\alpha^I \geq \underline{m} c^I$, with $\underline{m} = \min_\alpha(m_\alpha)$, and m_α is the number of node in area α.

We define the *area parameter δ* by

$$\delta = \frac{\max_{\alpha \in 1,\dots,r} \gamma_\alpha^E}{\underline{m} c^I} = \frac{\gamma^E}{\underline{m} c^I} \tag{2.5}$$

If condition $\delta \ll 1$ holds, it means that each area has dense internal connections and sparse external connections.

The two parameters d and δ characterize and quantify the trade-off between

connectivity inside the areas and among separate areas.

In this paper, we assume that the graph G is partitioned such that $d \ll 1$ and $\delta \ll 1$, see for instance the RTS 96 power network example in Figure 5.1, which accordingly to the weights on the connecting lines respects the conditions required.

We refer to Chow (1982); Chow et al. (1984) for constructive algorithms to identify such a partitioning.

We use the graph in Figure 2.1, to show a concrete example of the node and area parameter.

For simplicity we assume unitary weighted all the external connections and with weight 5 all the internal connections in the graph.
The graph has in total 13 nodes and three areas of $4, 5, 4$ nodes, respectively. In order to compute the node parameter we obtain $c^I = 1 \times 5$, $c^E = 1$ and it follows

$$d = \frac{c^E}{c^I} = 0.2. \tag{2.6}$$

Analogously, for the area parameter we obtain $\gamma^I = 4 \times 4$, $\underline{m} = 4$, $\gamma^E = 2 \times 1$ and it follows

$$\delta = \frac{\gamma^E}{\underline{m} c^I} = 0.1 \tag{2.7}$$

Both the parameters satisfy our requirements and the network has three internally dense, sparse connected areas.

2.3   Time-scale separation and singular perturbation analysis

In the following, we will focus on the first-order consensus dynamics (2.1) and decompose them into fast local dynamics within each area and network-wide slow motions between the areas. We will postpone the analysis of the second-order power network dynamics (2.2) to Chapter 4.

Slow inter-area motion To describe the slow inter-area motion, we define the *slow aggregate variable* $y_\alpha \in \mathbb{R}$ by the center of mass of area α:

$$y_\alpha = \sum_{i \in \mathcal{V}_\alpha} \frac{x_i^\alpha}{m_\alpha} = \frac{1}{m_\alpha} \mathbf{1}_{m_\alpha}^T x^\alpha, \quad \alpha \in \{1, \ldots, r\} \tag{2.8}$$

where x_i^α is the ith component of x for $i \in \mathcal{V}_\alpha$ and $x^\alpha = [x_1^\alpha, \ldots, x_{m_\alpha}^\alpha]^T$. Accordingly, $y \in \mathbb{R}^r$ is the concatenated vector of slow aggregate variables defined by

$$y = M_a^{-1} U^T x \tag{2.9}$$

where $M_a = \mathrm{diag}(m_1, \ldots, m_r) \in \mathbb{R}^{r \times r}$ and $U = \mathrm{blkdiag}(\mathbf{1}_{m_1}, \ldots, \mathbf{1}_{m_r}) \in \mathbb{R}^{n \times r}$.

Fast inner-area motion The fast inner-area motion is given by a weighted difference between the state of the nodes in each area, and different metrics have been proposed for this weighted difference Chow and Kokotović (1985); Bıyık and Arcak (2007). Here, we present the definition from Bıyık and Arcak (2007) and define the *fast local variable* $z_\alpha \in \mathbb{R}^{m_\alpha - 1}$ of area α as

$$z_\alpha = Q_\alpha x^\alpha, \quad \alpha \in 1, \ldots, r, \tag{2.10}$$

where the matrix $Q_\alpha \in \mathbb{R}^{m_\alpha - 1 \times m_\alpha}$ is defined by

$$Q_\alpha = \begin{bmatrix} -1 + (m_\alpha - 1)v & 1 - v & -v & \ldots & -v \\ -1 + (m_\alpha - 1)v & -v & 1 - v & \ldots & -v \\ \vdots & \vdots & \vdots & \ddots & \vdots \\ -1 + (m_\alpha - 1)v & -v & -v & \ldots & 1 - v \end{bmatrix} \tag{2.11}$$

with

$$v := \frac{m_\alpha - \sqrt{m_\alpha}}{m_\alpha(m_\alpha - 1)} < 1. \tag{2.12}$$

Accordingly, let $Q = \mathrm{blkdiag}(Q_1, \ldots, Q_r) \in \mathbb{R}^{n-r \times n}$, and let $z \in \mathbb{R}^{n-r}$ be the vector of fast variables z_α defined by

$$z = Qx \tag{2.13}$$

Compared to other choices of fast variables Chow and Kokotović (1985), the construction in (2.10) features the following convenient properties.

Lemma 2.3.1. *(Properties of Q_α)*

Consider the matrix Q_α in (2.10). The matrix Q_α features zero row sums and orthonormal rows, that is

$$Q_\alpha \mathbf{1}_{m_\alpha} = 0$$
$$Q_\alpha Q_\alpha^T = I_{m_\alpha - 1}.$$

In order to have a better understanding of what represent (2.13), we explicit z_i^α, which is the state referred to the $i-th$ node in area α, with $i \in \{1,\ldots,m_\alpha\}$.

$$
\begin{aligned}
z_i^\alpha &= x_i^\alpha - x_1^\alpha - v \sum_{j \in \mathcal{V}_\alpha} x_j^\alpha + m_\alpha v x_1^\alpha \\
&= x_i^\alpha - x_1^\alpha + v \sum_{j \in \mathcal{V}_\alpha} (m_\alpha x_1^\alpha - x_j^\alpha) \\
&= v \sum_{j \in \mathcal{V}_\alpha, j \neq i+1} (m_\alpha x_1^\alpha - x_j^\alpha) + (m_\alpha x_1^\alpha - x_i^\alpha)(v-1)
\end{aligned}
\tag{2.14}
$$

Therefore, each z_i^α is the sum of weighted differences between the first node and each other node within the area, weighting differently the difference which involves the $i-th$ node.

From (2.9) and (2.13), we obtain the transformation of the original state x into the aggregate and local variables:

$$
\begin{bmatrix} y \\ z \end{bmatrix} = \begin{bmatrix} C \\ Q \end{bmatrix} x,
\tag{2.15}
$$

where $C = M_a^{-1} U^T$. Due to Lemma 2.3.1, the inverse of the transformation (2.15) is explicitly given by

$$
x = \left(\begin{bmatrix} C \\ Q \end{bmatrix} \right)^{-1} \begin{bmatrix} y \\ z \end{bmatrix} = \begin{bmatrix} U & Q^T \end{bmatrix} \begin{bmatrix} y \\ z \end{bmatrix}
\tag{2.16}
$$

By means of the coordinate transformation (2.15)-(2.16), the dynamics (2.1) read in local and aggregate variables as

$$
\begin{bmatrix} \dot{y} \\ \dot{z} \end{bmatrix} = \begin{bmatrix} \overline{A}_{11} & \overline{A}_{12} \\ \overline{A}_{21} & \overline{A}_{22} \end{bmatrix} \begin{bmatrix} y \\ z \end{bmatrix},
\tag{2.17}
$$

where we used the fact that $L^I U = \mathbf{0}_n$ and the shorthands

$$
\begin{aligned}
\overline{A}_{11} &= -CL^E U, & \overline{A}_{12} &= -CL^E Q^T, \\
\overline{A}_{21} &= -QL^E U, & \overline{A}_{22} &= -Q(L^I + L^E)Q^T.
\end{aligned}
\tag{2.18}
$$

The submatrices in (2.18) are obtained using the Laplacian decomposition (2.3) and from the fact that C and U span the left and right nullspace of L^I, respectively.

Lemma 2.3.2. *(**Order relations I**)*
The ∞-norms (row sums) of the submatrices in (2.18) satisfy

$$
\begin{aligned}
\|\overline{A}_{11}\|_\infty &= \|CL^E U\|_\infty \in \mathcal{O}(c^I \delta), \\
\|\overline{A}_{12}\|_\infty &= \|CL^E Q^T\|_\infty \in \mathcal{O}(c^I \delta), \\
\|\overline{A}_{21}\|_\infty &= \|QL^E U\|_\infty \in \mathcal{O}(c^I d), \\
\|\overline{A}_{22}\|_\infty &= \|Q(L^I + L^E)Q^T\|_\infty \in \mathcal{O}(c^I)
\end{aligned}
$$

Proof. The order of the norms of submatrices $\overline{A}_{11}$, $\overline{A}_{12}$, and $\overline{A}_{21}$ can be proved analogous to Chow and Kokotović (1985).

   In the following we focus the submatrix $\overline{A}_{22}$. By construction in (2.18) and by applying the triangle inequality

$$
\|\overline{A}_{22}\|_\infty \leq \|QL^I Q^T\|_\infty + \|QL^E Q^T\|_\infty.
$$

The order of $\|QL^E Q^T\|_\infty$ can be proved noting from the definition of Laplacian matrix that $\|L^E\|_\infty = 2c^E$. Moreover, in Bıyık and Arcak (2007) it is proved that $\sqrt{2} \leq \|Q\|_\infty \leq 2$ and from (2.11) and (2.12) we can state that $1 \leq \|Q^T\|_\infty \leq \overline{m}$ with $\overline{m} = \max_\alpha\{m_\alpha\}$. Therefore it follows

$$
\|QL^E Q^T\|_\infty \leq \|Q\|_\infty \|L^E\|_\infty \|Q^T\|_\infty \leq 4\overline{m}c^E = 4\overline{m}c^I d.
$$

Regarding $\|QL^I Q^T\|_\infty$ we know, from the definition of Laplacian matrix, that $\|L^I\|_\infty = 2\overline{c}^I = 2kc^I$ where $\overline{c}^I = \max_{\alpha \in 1,\ldots,r, i \in \mathcal{V}_\alpha} c_{\alpha,i}^I$ and $k = \overline{c}^I/c^I > 1$. Thus, we obtain

$$
\|QL^I Q^T\|_\infty \leq \|Q\|_\infty \|L^I\|_\infty \|Q^T\|_\infty \leq 4\overline{m}kc^I.
$$

In Bıyık and Arcak (2007), it is shown that $\|QB^I\|_\infty > \tilde{c}^I$, where $\tilde{c}_{\alpha,i}^I$ is defined as the

number of internal links of node i in area α, $\tilde{c}^I = \min_{\alpha \in 1,\ldots,r, i \in \mathcal{V}_\alpha} \tilde{c}^I_{\alpha,i}$. Consequently, it holds that $\tilde{c}^I \geq c^I/\overline{\omega}$, and we obtain a lower bound of $\|QL^IQ^T\|_\infty$ as

$$\|QL^IQ^T\|_\infty = \|(QB^I)\operatorname{diag}(\{w_{ij}\}_{\{i,j\}\in\mathcal{E}_{\mathrm{int}}})(QB^I)^T\|_\infty$$
$$> \underline{\omega}\|QB^I(QB^I)^T\| > \underline{\omega}\tilde{c}^I \geq c^I\underline{\omega}/\overline{\omega}.$$

Since $\|QL^EQ^T\|_\infty \in \mathcal{O}(c^I d)$, since $\|QL^IQ^T\|_\infty \in \mathcal{O}(c^I)$, and since $d \ll 1$, we have that $\|A_{22}\|_\infty$ is of the same order as $\|QL^IQ^T\|_\infty$, namely $\mathcal{O}(c^I)$.

$\blacksquare$

In comparison with the corresponding result in Chow and Kokotović (1985), Lemma 2.3.2 provides an upper bound on $\|\overline{A}_{22}\|_\infty$ without additional assumptions, such as placing a lower bound on $|\mathcal{E}_\alpha|$. Specifically, they require that each node is connected to at least 3/4 of all the other nodes within the same area.

The order relations in Lemma 2.3.2 on the sub-matrices in the transformed dynamics (2.17) is helpful to our analyzis for several reasons:

- it determines a relation between the sub-matrices and the parameter d and δ;

- it guarantees for d and δ sufficiently small that the norms of $\overline{A}_{11}$, $\overline{A}_{12}$, $\overline{A}_{21}$ are smaller than the norm of $\overline{A}_{22}$;

- it suggests a two time-scale separation of the dynamics into the fast time scale
$$t_f = c^I t$$
and the slow time scale
$$t_s = \delta t_f = \delta c^I t;$$

- it suggests a rescaling of the submatrices as follows:

$$A_{11} = \frac{\overline{A}_{11}}{c^I \delta}, \qquad A_{12} = \frac{\overline{A}_{12}}{c^I \delta},$$
$$A_{21} = \frac{\overline{A}_{21}}{c^I d}, \qquad A_{22} = \frac{\overline{A}_{22}}{c^I}. \tag{2.19}$$

Notice that all sub-matrices A_{ij} are scale-free, that is, each $\|A_{ij}\|_\infty \in \mathcal{O}(1)$ for $i, j \in \{1, 2\}$. This means that the sub-matrices A_{ij} are (2.4) and (2.5) independent, they are not affected by variations of these two parameters.

Remark 2.3.3. The scale-free property of sub-matrices A_{ij} is a necessary condition because the singular perturbation analysis impose equal to zero the singular parameter which in our case is δ, see Khalil (2002). Therefore the sub-matrices in (2.17) cannot depend on this parameter.

Necessary condition for the future singular perturbation theorem 2.4.1 is the non singularity of A_{22}.

Lemma 2.3.4. *(Regularity)*
The matrix A_{22} is non-singular.

Proof. In order to show this property of A_{22} we show that it is strictly negative definite, which is a sufficient condition to have the invertibility of the matrix.

Since $L \succeq 0$, $L^I \succeq 0$, and $L^E \succeq 0$, we have that $QL^IQ^T \succeq 0$, $QL^EQ^T \succeq 0$, and $A_{22} = -Q(L^I + L^E)Q^T \preceq 0$.

Furthermore, since $\ker(L^I) = \ker(Q) = U$ and $\dim(\ker(L^I)) = \dim(\ker(Q)) = r$, we obtain $Q^T x \perp \ker(L^I)$ for each $x \in \mathbb{R}^{n-r}$ and $x^T QL^IQ^T x > 0$ for each $x \neq \mathbf{0}_{n-r}$. Thus, $QL^IQ^T > 0$ and $A_{22} = -Q(L^I + L^E)Q^T < 0$.

Consequently, A_{22} is nonsingular. ∎

In comparison to the analogous results in Chow and Kokotović (1985) and in Bıyık and Arcak (2007), Lemma 2.3.4 shows the non singularity of A_{22} without additional assumptions such as $d \ll 1$.

2.4 Singular Perturbation Analyzis

By rescaling the submatrices in (2.17) as in (2.19) and rescaling time as $t_s = \delta t_f$, the system (2.17) can be equivalently rewritten in *singular perturbation standard form*

$$\begin{cases} \dfrac{dy}{dt_s} = A_{11}y + A_{12}z\,, \\[2mm] \delta\dfrac{dz}{dt_s} = dA_{21}y + A_{22}z\,. \end{cases} \tag{2.20}$$

Considering the graph in Figure 2.1 its evolution on time assuming model (2.20) looks like Figure 2.3.
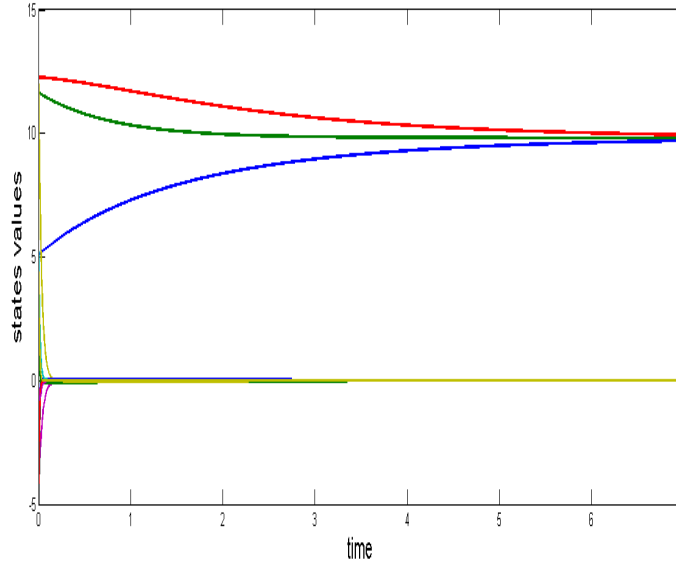
Figure 2.3: Evolution of the system in a singular perturbation standard form

We can see that the model induce three slow motions and several fast motions respect to the converging time. Indeed, the scope of the singular perturbation form is to determine a unique variable for each area, which approximate the motion of all the nodes within the area and the remaining variables describe the aggregation process of the nodes.

The standard singular perturbation analysis is rigorously explained in (Khalil, 2002, Section 11), here it is only reported the applicative aspect of that theory with the only scope to illustrate qualitatively the process. The reader is invited to deepen the study in the appropriate book.

Considering (2.20) we want to account as negligible the dynamic of the fast motion and therefore the singular perturbed parameter δ is imposed equal zero, which is an acceptable approximation because of $\delta \ll 1$. The second equation of (2.20) becomes an algebraic equation which has solution $z = -dA_{22}^{-1}A_{21}$ and replaced it in the first equation yields the slow reduced system (defined for the

slow aggregate variable y and in the scale t_s) as

$$\frac{dy_s}{dt_s} = (A_{11} - dA_{12}A_{22}^{-1}A_{21})y = A_0 y, \quad y_s(0) = y(0). \tag{2.21}$$

The corresponding fast boundary layer system (defined for the fast local variable z and in the scale t_f) is obtained as

$$\frac{dz_f}{dt_f} = A_{22}z, \quad z_f(0) = z(0) + dA_{22}^{-1}A_{21}y(0). \tag{2.22}$$

Tikhononov's Theorem (Khalil, 2002, Theorem 11.2) applied to the singularly perturbed system (2.20) then yields the following result.

Theorem 2.4.1. *(**Singular perturbation approximation I**) Consider the singularly perturbed system* (2.20) *with solution denoted by* $\big(y(t_s), z(t_s)\big)$, *the boundary layer system* (2.22) *with solution denoted by* $z_f(t_f)$, *as well as the slow reduced system* (2.21) *with solution* $y_s(t_s)$.

There exist $\delta^*, d^* > 0$ *such that for all* $0 < \delta \le \delta^*$, $0 < d \le d^*$ *the slow and fast motions of* (2.20) *are* (2.21) *and* (2.22), *respectively, and their solutions approximate the solution of* (2.20) *as follows:*

$$\begin{aligned}
y(t_s) &= y_s(t_s) + \mathcal{O}(\delta d), \\
z(t_s) &= -dA_{22}^{-1}A_{21}y_s(t_s) + z_f(t_f) + \mathcal{O}(\delta d).
\end{aligned} \tag{2.23}$$

Proof. The proof can be found in (Chow and Kokotović, 1985, Theorem 3.1). ∎

The statements of Theorem 2.4.1 are shown in Figure 2.4 with example in process of graph in Figure 2.1.

In Figure 2.4 are compared the evolution of (2.21), green lines and of (2.20) blue lines. There is almost an overlapping between (2.21) and the three slow motions of model (2.20), therefore the aggregate model in this case approximates precisely the full-order model. This means that the parameter δ and d are sufficiently small to have an acceptable error between the two systems.

The process described in this chapter and in particular Theorem 2.4.1 were already known in literature. Our work up-to-dated the notation used, improved the analyzis combining the analyzis of Chow and Kokotović (1985) and the definition
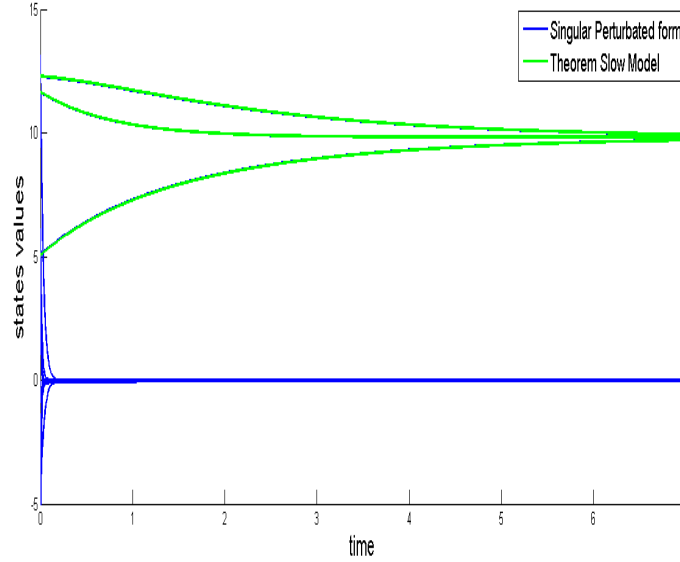
Figure 2.4: Comparison between the evolution of the slow approximating motion of the theorem and of the singular perturbation standard form

of fast motion defined in Bıyık and Arcak (2007) and relaxed both the assumptions to have A_{22} non singular and with infinite norm bounded.

The general idea of what we did so far can be summarized as:

$$\dot{x} = -Lx \implies \begin{cases} \dot{y} = A_{11}y + A_{12}z \\ \delta\dot{z} = A_{21}y + A_{22}z \end{cases} \implies \dot{y} = A_0 y$$

Thus is, starting from a Laplacian consensus dynamic of the first order with an high number of variables, possibly thousands or millions we achieved the singular perturbation standard form and we proved the existence of an approximating reduced-order model with possibly tens of variables.

The purpose of the Chapter 3 is to study the reduced-order model (2.21) obtained.

3

Properties of the Aggregate Model

In this Chapter, we analyze the properties of the aggregate model (2.21), where each area is collapsed into a single aggregate node.

In Chapter 2, we demonstrated the error order of the approximation of the full-order model with the aggregate model. Now we will characterize the aggregate model on its own.

3.1   Aggregate Model

The system matrix of the aggregate model (2.21) can be rewritten in an insightful way by defining

$$
\begin{aligned}
L_a &\triangleq U^T L^E U \,, \\
L_a^I &\triangleq U^T L^E Q^T (QLQ^T)^{-1} QL^E U \,, \\
L_{\mathrm{red}} &\triangleq L_a - L_a^I \,.
\end{aligned}
\tag{3.1}
$$

Lemma 3.1.1. (Reformulation of the aggregate model I)

The aggregate model (2.21) *reads equivalently as*

$$M_a \frac{dy_s}{dt} = -L_{\mathrm{red}}\, y_s\,.\tag{3.2}$$

Proof. The lemma follows from the identities

$$(c^I \delta) A_{11} = \bar{A}_{11} = -M_a^{-1}(U^T L^E U) = -M_a^{-1} L_a$$
$$(c^I \delta) d A_{12} A_{22}^{-1} A_{21} = = \bar{A}_{12} \bar{A}_{22}^{-1} \bar{A}_{21} = -M_a^{-1} U^T L^E Q^T (Q L Q^T)^{-1} Q L^E U$$
$$= -M_a^{-1} L_a^I\,.$$

which yield the system matrix

$$A_0 = \frac{\bar{A}_0}{c^I \delta} = -\frac{M_a^{-1} L_{\mathrm{red}}}{c^I \delta}\tag{3.3}$$

Replacing (3.3) in (2.21) and changing the time scale from t_s to t, system (3.2) follows. ∎

Notice that the aggregate model (3.2) is presented in time scale t. This formulation avoids the dependency on the parameter δ, and it will illuminate the connections between the aggregate model (3.2) and the original model (2.1).

An interesting result would be that reducing the order of the network, the system obtained still present a Laplacian consensus dynamic.
What we will see is that the aggregate model share many similarities with a Laplacian dynamics and it retains all the major properties.

3.2 Analyzis of the Aggregate Model State Matrix

The analyzis is organized as follows: matrices L_a and L_a^I are characterized singularly, then their properties are combined to define the matrix L_{red} and finally, we state a convergence result connecting the aggregate and the original model.

Definition 3.2.1 (Generalized Laplacian matrix).

Matrix $A \in \mathbb{R}^{n \times n}$ is a *generalized Laplacian matrix* if it is symmetric, positive

semidefinite, it features a simple zero eigenvalue and it has zero row and column sums.

Notice that a generalized Laplacian matrix necessarily has positive diagonal elements, but compared to a conventional Laplacian matrix it may have also positive off-diagonal elements corresponding to negatively weighted edges in the associated graph.

Theorem 3.2.2. (Characterisation of the matrices L_a and L_a^I)
Consider the matrices L_a, L_a^I defined in (3.1), *respectively. The following properties hold:*

1. *L_a is a Laplacian matrix;*

2. *L_a^I is a symmetric and positive semidefinite matrix with zero row and column sums.*

Proof. In order to prove the two statements we show that all the properties of the Laplacian matrix hold for L_a and for L_a^I hold only the listed properties.

- First, observe that $L^E \geq 0$ and $Q^T L Q > 0$, see the proof of Lemma 2.3.4. Since both matrices L_a and L_a^I in (3.1) are constructed as product matrices of the form $A^T B A$ with $B \geq 0$ and symmetric, it readily follows that both L_a and L_a^I are symmetric and positive semidefinite. In fact it holds that $A^T B A = A^T B^T A = (A^T B A)^T$.

- Second, since $L^E U \mathbf{1}_r = L^E \mathbf{1}_n = \mathbf{0}_n$, it follows that both L_a and L_a^I have zero row and column sums.

By now, we proved statement 2) and showed that L_a is symmetric, positive semidefinite matrices, and feature zero row and column sums.

- Third, consider a vector $x \in \mathbb{R}^r \setminus \text{span}(\mathbf{1}_r)$.

  Notice that $Ux = [x_1 \mathbf{1}_{m_1}^T, \ldots, x_r \mathbf{1}_{m_r}^T]^T \in \mathbb{R}^n$ and $Ux \in \text{span}(\mathbf{1}_n)$ if and only if $x \in \text{span}(\mathbf{1}_r)$. Since $\ker(L^E) = \text{span}(\mathbf{1}_n)$, it readily follows that $x = \mathbf{1}_r$ spans the nullspace of L_a, and the zero eigenvalue of L_a is simple.

- Furthermore, observe that the off-diagonals of L_a are non-positive. Thus, L_a is Laplacian matrix. This completes the proof of statement 1).

■

Remark 3.2.3. We like to show the reader that, adding an assumption to the analyzis, theorem 3.2.2 can be extended proving that the vector $x = \mathbf{1}_r$ is the eigenvector for L_a^I referred to the simple zero eigenvalue.

Assume that at least one node in the graph does not have any external connection. Likewise to the third point of the proof of theorem 3.2.2 we obtain:

$$L^E U x = \begin{bmatrix} \sum_{i=1}^r x_i \sum_{j \in \mathcal{V}_i} L_{1,j}^E \\ \vdots \\ \sum_{i=1}^r x_i \sum_{j \in \mathcal{V}_r} L_{r,j}^E \end{bmatrix}. \tag{3.4}$$

Due to the assumption at least one row of L^E is of all zero, therefore there is at least one zero element in (3.4). Moreover, for the connectivity of the graph in the same area of that node there is at least one node with an external connection, therefore there is at least one non zero element in (3.4). We can now conclude that $L^E U x \notin \text{columnspan}(U)$.

Matrix L_a^I is a generalized Laplacian matrix.

The assumption made is really general and it probably holds for many of the large-scale networks characterised as Section 2.2 requires. Whereas, the property of L_a^I achieved is not necessary for our work, therefore we decided to not add an usefulness assumption. Anyway this property could be useful for further analyzis. □

In the following, we term the matrix $L_{\text{red}} = L_a - L_a^I$ in (3.2) as the *reduced Laplacian matrix*. This terminology is justified by the following results.

Theorem 3.2.4. *The* Reduced Laplacian Matrix L_{red} *defined in* (3.1) *is a generalized Laplacian matrix.*

Proof. The proof that L_{red} is symmetric and feature zero row and column sums follow readily from theorem 3.2.2.

In order to prove positive semidefiniteness of L_{red} and that it features a simple zero eigenvalue, we invert the coordinate transformation (2.15)-(2.16) to obtain

$$-L = \begin{bmatrix} U & Q^T \end{bmatrix} \bar{A} \begin{bmatrix} M_a^{-1} U^T \\ Q \end{bmatrix} = \begin{bmatrix} M_a^{-1} U^T \\ Q \end{bmatrix}^T F \begin{bmatrix} M_a^{-1} U^T \\ Q \end{bmatrix},$$

where we defined $F = \text{blkdiag}(M_a, I_{(n-r)\times(n-r)})\bar{A}$. Notice that F is necessarily symmetric since it is congruent to L. Since $-L \leq 0$ with simple zero eigenvalue and since the matrix $[UM_a^{-1}, Q^T]$ is of full rank (it equals the transpose of the nonsingular transformation matrix in (2.15)), we obtain that $F \leq 0$ and F features a simple zero eigenvalue.

Next, recall that the Schur complement of $\bar{A}$ with respect to its (2,2)-block equals $-M_a^{-1}L_{\text{red}}$:

$$\overline{A}_{11} - \overline{A}_{12}\overline{A}_{22}^{-1}\overline{A}_{21} = -(CL^E U - CL^E Q^T(Q(L)Q^T)^{-1}QL^E U) = -M_a^{-1}L_{\text{red}}.$$

Thus, the Schur complement of F with respect to its (2,2)-block equals $-L_{\text{red}}$, that is, $F_{11} - F_{12}F_{22}^{-1}F_{21} = -L_{\text{red}}$.

Since F is negative semidefinite, it follows by the closure properties of the Schur complement (Zhang, 2005, Chapter 4) that its Schur complement is negative semidefinite as well.

Furthermore, the Haynsworth inertia additivity formula (Zhang, 2005, Equation (0.10.1)) yields that the inertia of the matrix F (that is, the number of positive, negative, and zero eigenvalues) equal the inertia of F_{22} plus the inertia of its Schur complement $F_{11} - F_{12}F_{22}^{-1}F_{21}$. Since F_{22} is nonsingular, it necessarily follows that the Schur complement $F_{11} - F_{12}F_{22}^{-1}F_{21} = -L_{\text{red}}$ features exactly one zero eigenvalue.

In summary, L_{red} is symmetric, it has zero row and column sums, and it is positive semidefinite with simple zero eigenvalue. Hence, L_{red} is a generalized Laplacian matrix.

∎

Remark 3.2.5. (**Graphs associated to the reduced Laplacian matrices**) The reduced Laplacian is obtained as the difference of the Laplacians L_a and L_a^I. The matrix L_a is the Laplacian corresponding to the aggregate graph, where each area is collapsed into a single node.

The matrix L_a^I shows the contribution of the area-internal topology and weights to the reduced Laplacian L_{red}. Whereas L_a is a Laplacian matrix with positive edge weights, the matrix L_a^I itself as well as L_{red} can possibly feature negative edge weights. Hence, the reduced system can possibly feature adverse interactions.

$\square$

So far, we identified the aggregate model (2.21) as a generalized Laplacian dynamics which share several properties with the Laplacian dynamics of the full-order model (2.1). This identification allow us to use the known results for these consensus dynamics which can be find for example in Olfati-Saber et al. (2007) and yield the following asymptotic convergence result.

Corollary 3.2.6. *(Consensus convergence)*
Consider the aggregate model (3.2) *and the original consensus model* (2.1).
The following statements hold:

1. *The aggregate model* (3.2) *synchronizes exponentially to*

$$y_{s\infty} \cdot \mathbf{1}_r = \frac{\sum_{\alpha=1}^r m_\alpha y_\alpha(0)}{\sum_{\alpha=1}^r m_\alpha} \cdot \mathbf{1}_r.$$

2. *The consensus model* (2.1) *synchronizes exponentially to*

$$x_\infty \cdot \mathbf{1}_n = \frac{\sum_{i=1}^n x_i(0)}{n} \cdot \mathbf{1}_n.$$

Moreover, we have that $y_{s\infty} = x_\infty$.

Proof. Theorem 3.2.2 implies stability of the aggregate model (3.2) with respect to the agreement subspace $\mathbf{1}_r$. To find the particular consensus value $y_{s\infty}$, we pre-multiply the model (3.2) on both sides by the vector $\mathbf{1}_r^T$. By considering the Laplacian properties $\mathbf{1}_r^T L_{\mathrm{red}} = \mathbf{0}_r^T$, we arrive at $\mathbf{1}_r^T M_a \dot{y}_s(t) = 0$, or equivalently

$$\mathbf{1}_r^T M_a y_s(t) = \sum_{\alpha=1}^r m_\alpha y_{s\alpha}(t) = const. \quad \forall\, t \geq 0.$$

By equalizing the previous equation for the two particular cases $t = 0$ and $t \to \infty$, we obtain

$$\sum_{\alpha=1}^r m_\alpha y_{s\alpha}(0) = \sum_{\alpha=1}^r m_\alpha y_{s\alpha}(t \to \infty).$$

Thus, we obtain the explicit consensus point

$$\lim_{t\to\infty} y_s(t) = y_{s\infty} = \frac{\sum_{\alpha=1}^r m_\alpha y_{s\alpha}(0)}{\sum_{\alpha=1}^r m_\alpha} \tag{3.5}$$

The same analogous reasoning applied to (2.1) yields that

$$\lim_{t \to \infty} x(t) = x_\infty = \frac{\sum_{i=1}^{n} x_i(0)}{n}$$

Finally, the equality $y_{s\infty} = x_\infty$ follows from the calculation

$$
\begin{aligned}
y_{s\infty} &= \frac{\sum_{\alpha=1}^{r} m_\alpha y_\alpha(0)}{\sum_{\alpha=1}^{r} m_\alpha} = \frac{\sum_{\alpha=1}^{r} m_\alpha \sum_{j \in \mathcal{V}_\alpha} \frac{x_j^\alpha(0)}{m_\alpha}}{\sum_{\alpha=1}^{r} m_\alpha} \\
&= \frac{\sum_{\alpha=1}^{r} \sum_{j \in \mathcal{V}_\alpha} x_j^\alpha(0)}{\sum_{\alpha=1}^{r} m_\alpha} = \frac{\sum_{i=1}^{n} x_i(0)}{n} = x_\infty,
\end{aligned}
$$

where we applied definition (2.8) in the second equality. ∎

Notice that Theorem 2.4.1 and Corollary 3.2.6 together guarantee that at each instant, in the infinite interval of time, the full-order system (2.20) and the aggregate model (3.2) cannot be far one to each arbitrarily. This gives intuitively a condition also in the rate of convergence of the two systems. The difference between the time needed by system (2.20) and system (3.2) to reach the consensus is $O(\delta d)$.

The analyzis of the graphs modelled with dynamic (2.1) is yet complete. Chapter 4 is dedicated on the analyzis of mechanical swing dynamics (2.2).

4

Aggregation in Power Networks

In the following chapter, we extend the results derived in the Chapters 2 and 3 from the first-order consensus system (2.1) to the second-order system (2.2), which models the electromechanical swing dynamics of an interconnected power grid.

Using the same order utilized in Chapters 2 and 3, we will face several mathematical issues arising from the complex dynamics involved. In the following, we focus more on how to solve these mathematical issues than explaining redundantly why we do each step.

4.1   Singular Perturbation Analyzis

Analogous to Section 2.2, we define the quantities d and δ as in (2.4) and (2.5). We deviate from the first-order model (2.1) by accounting for different generator inertia coefficients, and we define the slow aggregate variable by

$$y = C_a x = M_a^{-1} U^T M x,$$

where the matrices M_a and C_a are redefined as follows

$$M_a \triangleq U^T M U \quad \text{and} \quad C_a = M_a^{-1} U^T M$$

Thus, y_α corresponds to the *center of inertia angle* of the area α. We maintain the fast local variable $z = Qx$ and obtain

$$\begin{bmatrix} y \\ z \end{bmatrix} = \begin{bmatrix} C_a \\ Q \end{bmatrix} x \quad , \quad \begin{bmatrix} \dot{y} \\ \dot{z} \end{bmatrix} = \begin{bmatrix} C_a \\ Q \end{bmatrix} \dot{x}.$$

The inverse coordinate transformation then reads as

$$x = \begin{bmatrix} U & M^{-1} Q^T (Q M^{-1} Q^T)^{-1} \end{bmatrix} \begin{bmatrix} y \\ z \end{bmatrix}.$$

This inverse transformation is the extension of (2.16) accounting for non-identical inertia coefficients, and it has been presented in Date and Chow (1991) with a different matrix Q.

Accordingly, we also define the diagonal matrix

$$D_a \triangleq U^T D U \ \in \mathbb{R}^{r \times r} \tag{4.1}$$

representing the aggregate damping of each area.

The power network dynamics (2.2) can then be equivalently reformulated in the fast and slow variables as

$$
\begin{bmatrix} \ddot{y} \\ \ddot{z} \end{bmatrix} = \begin{bmatrix} C_a \\ Q \end{bmatrix} \ddot{x} = \begin{bmatrix} C_a \\ Q \end{bmatrix} \left[-M^{-1}D\dot{x} - M^{-1}Lx \right]
$$

$$
= \begin{bmatrix} C_a \\ Q \end{bmatrix} \left(-M^{-1}D \begin{bmatrix} U & M^{-1}Q^T(QM^{-1}Q^T)^{-1} \end{bmatrix} \begin{bmatrix} \dot{y} \\ \dot{z} \end{bmatrix} \right.
$$

$$
\left. -M^{-1}L \begin{bmatrix} U & M^{-1}Q^T(QM^{-1}Q^T)^{-1} \end{bmatrix} \begin{bmatrix} y \\ z \end{bmatrix} \right)
$$

$$
= - \begin{bmatrix} C_aM^{-1}DU & C_aM^{-1}DM^{-1}Q^T(QM^{-1}Q^T)^{-1} \\ QM^{-1}DU & QM^{-1}DM^{-1}Q^T(QM^{-1}Q^T)^{-1} \end{bmatrix} \begin{bmatrix} \dot{y} \\ \dot{z} \end{bmatrix}
$$

$$
- \begin{bmatrix} C_aM^{-1}LU & C_aM^{-1}LM^{-1}Q^T(QM^{-1}Q^T)^{-1} \\ QM^{-1}LU & QM^{-1}LM^{-1}Q^T(QM^{-1}Q^T)^{-1} \end{bmatrix} \begin{bmatrix} y \\ z \end{bmatrix} \tag{4.2}
$$

$$
= - \begin{bmatrix} M_a^{-1}D_aC_aU & M_a^{-1}D_aC_aM^{-1}Q^T(QM^{-1}Q^T)^{-1} \\ QM^{-1}DU & QM^{-1}DQ^T \end{bmatrix} \begin{bmatrix} \dot{y} \\ \dot{z} \end{bmatrix}
$$

$$
- \begin{bmatrix} M_a^{-1}U^TLU & M_a^{-1}U^TLM^{-1}Q^T(QM^{-1}Q^T)^{-1} \\ QM^{-1}L^EU & QLM^{-1}Q^T(QM^{-1}Q^T)^{-1} \end{bmatrix} \begin{bmatrix} y \\ z \end{bmatrix}
$$

$$
= - \begin{bmatrix} M_a^{-1}D_a & 0_{r\times(n-r)} \\ QM^{-1}DU & QM^{-1}DQ^T \end{bmatrix} \begin{bmatrix} \dot{y} \\ \dot{z} \end{bmatrix}
$$

$$
- \begin{bmatrix} M_a^{-1}L_a & M_a^{-1}U^TL^EM^{-1}Q^T(QM^{-1}Q^T)^{-1} \\ QM^{-1}L^EU & QM^{-1}LM^{-1}Q^T(QM^{-1}Q^T)^{-1} \end{bmatrix} \begin{bmatrix} y \\ z \end{bmatrix}
$$

Where are used the following simplifying identities

$$
C_aM^{-1}D = M_a^{-1}D_aC_a,
$$
$$
C_aU = I_r,
$$
$$
QU = \mathbf{0}_{n-r\times r}.
$$

The submatrices which multiply the vector $\left[y^T, z^T \right]^T$ in (4.2) have a similar structure to those in (2.18). To see this, analogously to matrix Q, we define

$$
\tilde{Q} \triangleq (QM^{-1}Q^T)^{-1}Q
$$

satisfying similar properties

$$QM^{-1}\tilde{Q}^T = I_{n-r}$$
$$\tilde{Q}U = 0_{n-r\times r}.$$

The definition of the submatrices follows

$$\tilde{A}_{11} = \frac{-M_a^{-1}L_a}{c^I\delta}, \quad \tilde{A}_{12} = \frac{-M_a^{-1}U^TL^EM^{-1}\tilde{Q}^T}{c^I\delta}$$
$$\tilde{A}_{21} = \frac{-QM^{-1}L^EU}{c^Id}, \quad \tilde{A}_{22} = \frac{-QM^{-1}LM^{-1}\tilde{Q}^T}{c^I}. \tag{4.3}$$

These matrices share several properties with the correspondent for the first-order case, some of them are stated in the following lemma.

Lemma 4.1.1. *(**Order relations and regularity II**) The ∞-norms (row sums) of the submatrices in* (4.3) *satisfies*

$$\|\tilde{A}_{11}\|_\infty \in \mathcal{O}(c^I\delta),$$
$$\|\tilde{A}_{12}\|_\infty \in \mathcal{O}(c^I\delta),$$
$$\|\tilde{A}_{21}\|_\infty \in \mathcal{O}(c^Id),$$
$$\|\tilde{A}_{22}\|_\infty \in \mathcal{O}(c^I).$$

Moreover, the matrix $\tilde{A}_{22}$ is non-singular.

Proof. Notice that the $\infty-$norm of $\tilde{Q}^T$ is upper bounded by a constant since $\tilde{Q}^T$ is the product of constant $\infty-$norms matrices. Moreover, we have that $\ker(\tilde{Q}) = \ker(Q)$. The proof of Lemma 4.1.1 follows then along analogous lines as the proofs of Lemma 2.3.2 and 2.3.4. ∎

Analogous to the first-order system (2.1), we apply a change of time scale to bring the model (4.2) to singular perturbation standard form. For the double integrator system (4.2), the time scales to describe the fast and the slow motion are

$$t_f = c^I t \quad , \quad t_s = \sqrt{\delta}t_f = \sqrt{\delta}c^I t.$$

The natural procedure for what we have seen in Chapter (2) is to rewrite system

(4.2) in an explicit singular perturbation form. Whereas, for a second-order system this form cannot be achieved directly, the system is rewritten in a state space form and several mathematical issues appears. For the best of our knowledge (4.2) has never been identified as a singular perturbed system.

Lemma 4.1.2. *(***Power network model in singular perturbation standard form***)* *Consider the power network dynamics* (2.2) *rewritten as in* (4.2)*, the matrices in* (4.3) *and the parameters δ and d defined in* (2.5) *and in* (2.4)*, respectively. System* (4.2) *then reads equivalently as*

$$
\frac{d}{dt_s}
\begin{bmatrix} \bar{y} \\ \dot{\bar{y}} \\ \sqrt{\delta}z \\ \sqrt{\delta}\dot{z} \end{bmatrix}
=
\begin{bmatrix}
0 & \frac{I_r}{c^I} & 0 & 0 \\
\tilde{A}_{11} & -\tilde{D}_1 & \tilde{A}_{12} & 0 \\
0 & 0 & 0 & \frac{I_{n-r}}{c^I} \\
d\tilde{A}_{21} & -\frac{\sqrt{\delta}QM^{-1}DU}{c^I} & \tilde{A}_{22} & -\frac{QM^{-1}DQ^T}{c^I}
\end{bmatrix}
\begin{bmatrix} \bar{y} \\ \dot{\bar{y}} \\ z \\ \dot{z} \end{bmatrix},
\tag{4.4}
$$

where $[\bar{y}^T, \dot{\bar{y}}^T]^T = [y^T, \dot{y}^T/\sqrt{\delta}]^T$ and the submatrix $\tilde{D}_1 = \frac{M_a^{-1}D_a}{c^I\sqrt{\delta}}$ converges to a bounded and positive definite diagonal matrix as $\delta \to 0$.

Proof. The proof consist of two main steps, in the first one is shown the computation which yields system (4.2) to the form (4.4), in the second one it is proved the limit boundedness of $\tilde{D}_1$ and of matrix $\frac{\sqrt{\delta}QM^{-1}DU}{c^I}$.

Regarding the first step.

System (4.2) written in state space form reads

$$
\frac{d}{dt}
\begin{bmatrix} y \\ z \\ \dot{y} \\ \dot{z} \end{bmatrix}
=
\begin{bmatrix}
0_r & 0_{r\times n-r} & I_r & 0_{r\times n-r} \\
0_{n-r\times r} & 0_{n-r} & 0_{n-r\times r} & I_{n-r} \\
c^I\delta\tilde{A}_{11} & c^I\delta\tilde{A}_{12} & -M_a^{-1}D_a & 0_{r\times n-r} \\
c^I d\tilde{A}_{21} & c^I\tilde{A}_{22} & -QM^{-1}DU & -QM^{-1}DQ^T
\end{bmatrix}
\begin{bmatrix} y \\ z \\ \dot{y} \\ \dot{z} \end{bmatrix}
$$

Changing the time-scale in $t_s = \sqrt{\delta}c^I t$, we arrive at

$$
\frac{d}{dt_s}
\begin{bmatrix} y \\ z \\ \dot{y} \\ \dot{z} \end{bmatrix}
=
\begin{bmatrix}
0_r & 0_{r\times n-r} & I_r & \frac{I_r}{c^I\sqrt{\delta}} & 0_{r\times n-r} \\
0_{n-r\times r} & 0_{n-r} & 0_{n-r\times r} & \frac{I_{n-r}}{c^I\sqrt{\delta}} \\
\sqrt{\delta}\tilde{A}_{11} & \sqrt{\delta}\tilde{A}_{12} & -\frac{M_a^{-1}D_a}{c^I\sqrt{\delta}} & 0_{r\times n-r} \\
\frac{d\tilde{A}_{21}}{\sqrt{\delta}} & \frac{\tilde{A}_{22}}{\sqrt{\delta}} & -\frac{QM^{-1}DU}{c^I\sqrt{\delta}} & -\frac{QM^{-1}DQ^T}{c^I\sqrt{\delta}}
\end{bmatrix}
\begin{bmatrix} y \\ z \\ \dot{y} \\ \dot{z} \end{bmatrix}
$$

The slow and fast variable corresponds to the concatenated vectors $\left[y^T, \dot{y}^T\right]^T$ and $\left[z^T, \dot{z}^T\right]^T$ respectively. The system can be rewritten pre-multiplying the fast variable by the singular perturbation parameter $\sqrt{\delta}$.

$$
\frac{d}{dt_s}\begin{bmatrix} y \\ \sqrt{\delta}z \\ \dot{y} \\ \sqrt{\delta}\dot{z} \end{bmatrix} = \begin{bmatrix} 0_r & 0_{r\times n-r} & \frac{I_r}{c^I\sqrt{\delta}} & 0_{r\times n-r} \\ 0_{n-r\times r} & 0_{n-r} & 0_{n-r\times r} & \frac{I_{n-r}}{c^I} \\ \sqrt{\delta}\tilde{A}_{11} & \sqrt{\delta}\tilde{A}_{12} & -\frac{M_a^{-1}D_a}{c^I\sqrt{\delta}} & 0_{r\times n-r} \\ d\tilde{A}_{21} & \tilde{A}_{22} & -\frac{QM^{-1}DU}{c^I} & -\frac{QM^{-1}DQ^T}{c^I} \end{bmatrix}\begin{bmatrix} y \\ z \\ \dot{y} \\ \dot{z} \end{bmatrix}
$$

The dependency on δ of the matrix of the system results incompatible with the singular perturbation theory which impose $\delta = 0$. The problem is solved with a change of the reference frame.

Applying a general diagonal change of coordinates as:

$$
\begin{bmatrix} \bar{y} \\ \bar{z} \\ \dot{\bar{y}} \\ \dot{\bar{z}} \end{bmatrix} = \begin{bmatrix} a & 0 & 0 & 0 \\ 0 & b & 0 & 0 \\ 0 & 0 & e & 0 \\ 0 & 0 & 0 & f \end{bmatrix}\begin{bmatrix} y \\ z \\ \dot{y} \\ \dot{z} \end{bmatrix} = \begin{bmatrix} ay \\ bz \\ e\dot{y} \\ f\dot{z} \end{bmatrix}
$$

where a, b, e, f are three arbitrary constants, we obtain:

$$
\frac{d}{dt_s}\begin{bmatrix} \bar{y} \\ \sqrt{\delta}\bar{z} \\ \dot{\bar{y}} \\ \sqrt{\delta}\dot{\bar{z}} \end{bmatrix} = \begin{bmatrix} 0 & 0 & \frac{aI_r}{ec^I\sqrt{\delta}} & 0 \\ 0 & 0 & 0 & \frac{bI_{n-r}}{fc^I} \\ \frac{e\sqrt{\delta}\tilde{A}_{11}}{a} & \frac{e\sqrt{\delta}\tilde{A}_{12}}{b} & -\frac{M_a^{-1}D_a}{c^I\sqrt{\delta}} & 0 \\ \frac{df\tilde{A}_{21}}{a} & \frac{f\tilde{A}_{22}}{b} & \underline{0} & -\frac{QDQ^T}{c^I} \end{bmatrix}\begin{bmatrix} \bar{y} \\ \bar{z} \\ \dot{\bar{y}} \\ \dot{\bar{z}} \end{bmatrix}
$$

The solution $a = b = f = 1$, $e = \frac{1}{\sqrt{\delta}}$ corresponding to the change of variables

$$
\begin{bmatrix} \bar{y}^T & z^T & \dot{\bar{y}}^T & \dot{z}^T \end{bmatrix}^T = \begin{bmatrix} y^T & z^T & \dot{y}^T/\sqrt{\delta} & \dot{z}^T \end{bmatrix}^T
$$

.

simplifies the dependency on $\sqrt{\delta}$ of almost all the submatrices and results in

system

$$\frac{d}{dt_s}\begin{bmatrix} \bar{y} \\ \sqrt{\delta}\bar{z} \\ \dot{\bar{y}} \\ \sqrt{\delta}\dot{\bar{z}} \end{bmatrix} = \begin{bmatrix} 0 & 0 & \frac{I_r}{c^I} & 0 \\ 0 & 0 & 0 & \frac{I_{n-r}}{c^I} \\ \tilde{A}_{11} & \tilde{A}_{12} & -\frac{M_a^{-1}D_a}{c^I\sqrt{\delta}} & \underline{0} \\ d\tilde{A}_{21} & \tilde{A}_{22} & -\frac{\sqrt{\delta}QM^{-1}DU}{c^I} & -\frac{QM^{-1}DQ^T}{c^I} \end{bmatrix}\begin{bmatrix} \bar{y} \\ \bar{z} \\ \dot{\bar{y}} \\ \dot{\bar{z}} \end{bmatrix}$$

which yields (4.4).

Regarding the second step.

In the following, we show that the two submatrices

$$\tilde{D}_1 = \frac{M_a^{-1}D_a}{c^I\sqrt{\delta}} \quad , \quad \tilde{D}_2 = \frac{\sqrt{\delta}QM^{-1}DU}{c^I}$$

remain bounded as $\delta \to 0$.

Clearly, we have that $\tilde{D}_2 \to 0$ when $\delta \to 0$ since $\sqrt{\delta}/c^I \to 0$ and $QM^{-1}DU$ does not depend on δ. In the following, we show that the submatrix $\tilde{D}_1$ converges to a bounded and positive definite diagonal matrix $K \in \mathbb{R}^{r \times r}$ as $\delta \to 0$.

The problem is that δ is composed by three parameters which affect $\tilde{D}_1$ differently, therefore the analyzis must be extended to the asymptotic variation of each parameter. We substitute the definition of δ in $\tilde{D}_1$ and obtain

$$\tilde{D}_1 = \frac{M_a^{-1}D_a}{c^I\sqrt{\delta}} = \frac{\sqrt{m}}{\sqrt{c^I}\sqrt{\gamma^E}}M_a^{-1}D_a \,.$$

Notice that the diagonal positive definite matrix $M_a^{-1}D_a$ does not depend on δ and it does not affect the asymptotic behaviour.

The limit $\delta \to 0$ is equivalent to at least one of three possible limit processes:

$$\delta \to 0 \quad \Longleftrightarrow \quad \begin{cases} \gamma^E \to 0 \\ \underline{m} \to \infty \\ c^I \to \infty \end{cases} \tag{4.5}$$

Recall the lower and upper bound of these three parameters:

$$\underline{w} < c^I < \underline{m}\,\overline{w}, \tag{4.6a}$$

$$c^I/\overline{w} < \underline{m} < c^I\overline{w}, \tag{4.6b}$$

$$\underline{w} < \gamma^E \ll \underline{m}c^I, \tag{4.6c}$$

where (4.6a)-(4.6b) follow from the definition of c^I, and (4.6c) follows from the definition of γ^E and the condition $\delta \ll 1$.

The convergence $\tilde{D}_1 \to K$ is proved by contradiction in two steps. First, assume that $\tilde{D}_1$ converges to the zero matrix, then, at least one of the following conditions must occur:

$$\tilde{D}_1 \to 0 \quad \Longleftrightarrow \quad \begin{cases} \gamma^E \to \infty \\ \underline{m} \to 0 \\ c^I \to \infty \end{cases} \tag{4.7}$$

The first two cases in (4.7) can be discarded since they contradict hypothesis (4.5). The third case can be discarded, since inequality (4.6a) shows that $c^I \to \infty$ implies that $\sqrt{\underline{m}/c^I}$ becomes constant. Thus, we conclude that $\tilde{D}_1$ does not converge to the zero matrix as $\delta \to 0$.

Next, assume that the diagonal elements of $\tilde{D}_1$ diverge, then at least one of the following conditions must occur:

$$\tilde{D}_1 \to \infty \quad \Longleftrightarrow \quad \begin{cases} \gamma^E \to 0 \\ \underline{m} \to \infty \\ c^I \to 0 \end{cases} \tag{4.8}$$

The first and the third conditions can be discarded since they contradict (4.5), (4.6a), and (4.6c). The second condition can be discarded since (4.6b) shows that $\sqrt{\underline{m}/c^I}$ must be a finite number.

Thus, $\tilde{D}_1$ does not diverge as $\delta \to 0$.   ∎

System (4.4) has the same structure as system (2.20), and a singular perturba-

tion analysis yields the slow reduced system

$$\frac{d}{dt_s}\begin{bmatrix}\bar{y}_s \\ \dot{\bar{y}}_s\end{bmatrix} = (R_{11} - R_{12}R_{22}^{-1}R_{21})s = \begin{bmatrix}0 & \frac{I_r}{c^I} \\ \tilde{A}_0 & -\bar{D}_1\end{bmatrix}\begin{bmatrix}\bar{y}_s \\ \dot{\bar{y}}_s\end{bmatrix},$$

$$[\bar{y}_s(0)\ \dot{\bar{y}}_s(0)]^T = [\bar{y}(0)\ \dot{\bar{y}}(0)]^T, \tag{4.9}$$

where $\tilde{A}_0 = \tilde{A}_{11} - d\tilde{A}_{12}\tilde{A}_{22}^{-1}\tilde{A}_{21}$, $\bar{D}_1 = \lim_{\delta \to 0}\frac{M_a^{-1}D_a}{c^I\sqrt{\delta}}$ is a bounded and positive definite diagonal matrix, and

$$R_{11} = \begin{bmatrix}0 & \frac{I_r}{c^I} \\ \tilde{A}_{11} & -\bar{D}_1\end{bmatrix}, \quad R_{12} = \begin{bmatrix}0 & 0 \\ \tilde{A}_{12} & 0\end{bmatrix},$$

$$R_{21} = \begin{bmatrix}0 & 0 \\ d\tilde{A}_{21} & 0\end{bmatrix}, \quad R_{22} = \begin{bmatrix}0 & \frac{I_{n-r}}{c^I} \\ \tilde{A}_{22} & -\frac{QM^{-1}DQ^T}{c^I}\end{bmatrix}.$$

The corresponding fast boundary layer system is obtained as

$$\frac{d}{dt_s}\begin{bmatrix}z_f \\ \dot{z}_f\end{bmatrix} = R_{22}\begin{bmatrix}z_f \\ \dot{z}_f\end{bmatrix}$$

$$\begin{bmatrix}z_f(0) \\ \dot{z}_f(0)\end{bmatrix} = \begin{bmatrix}z(0) \\ \dot{z}(0)\end{bmatrix} + dR_{22}^{-1}R_{21}\begin{bmatrix}\bar{y}(0), \\ \dot{\bar{y}}(0)\end{bmatrix}. \tag{4.10}$$

The analog of Theorem 2.4.1 is then as follows:

Theorem 4.1.3. *(**Singular perturbation approximation II**) Consider the singularly perturbed system (4.4) with solution denoted by $\left(\bar{y}(t_s), \dot{\bar{y}}(t_s), z(t_s), \dot{z}(t_s)\right)$, the boundary layer system (4.10) with solution denoted by $z_f(t_f), \dot{z}_f(t_f)$, as well as the slow reduced system (4.9) with solution $\bar{y}_s(t_s), \dot{\bar{y}}_s(t_s)$.*

There exist $\delta^*, d^* > 0$ such that for all $0 < \delta \leq \delta^*$, $0 < d \leq d^*$ the slow and fast motions of (4.4) are (4.9) and (4.10), respectively, and their solutions approximate

the solution of (4.4) *as follows:*

$$
\begin{bmatrix} \bar{y}(t_s) \\ \dot{\bar{y}}(t_s) \end{bmatrix} = \begin{bmatrix} \bar{y}_s(t_s) \\ \dot{\bar{y}}_s(t_s) \end{bmatrix} + \mathcal{O}(\sqrt{\delta}d),
$$

$$
\begin{bmatrix} z(t_s) \\ \dot{z}(t_s) \end{bmatrix} = dR_{22}^{-1}R_{21} \begin{bmatrix} \bar{y}_s(t_s) \\ \dot{\bar{y}}_s(t_s) \end{bmatrix} + \begin{bmatrix} z_f(t_f) \\ \dot{z}_f(t_f) \end{bmatrix} + \mathcal{O}(\sqrt{\delta}d), \tag{4.11}
$$

$$
= \begin{bmatrix} -d\tilde{A}_{22}^{-1}\tilde{A}_{21} & 0 \\ 0 & 0 \end{bmatrix} \begin{bmatrix} \bar{y}_s \\ \dot{\bar{y}}_s \end{bmatrix} + \begin{bmatrix} z_f(t_f) \\ \dot{z}_f(t_f) \end{bmatrix} + \mathcal{O}(\sqrt{\delta}d). \tag{4.12}
$$

Proof. The proof coincide with the proof of Theorem 2.4.1 ∎

The resulting equation (4.11) and (4.12) of theorem (4.1.3) show nicely the analogy to the singular perturbation of the first order, but they can be rewritten in a more clear form as

$$
y(t_s) = y_s(t_s) + \mathcal{O}(\sqrt{\delta}d),
$$
$$
\dot{y}(t_s) = \dot{y}_s(t_s) + \mathcal{O}(\sqrt{\delta}d),
$$
$$
z(t_s) = -d\tilde{A}_{22}^{-1}\tilde{A}_{21}y_s(t_s) + z_f(t_f) + \mathcal{O}(\sqrt{\delta}d)
$$
$$
\dot{z}(t_s) = \dot{z}_f(t_f) + \mathcal{O}(\sqrt{\delta}d)
$$

The statements of Theorem 4.1.3 are shown in Figures 4.1, proceeding the example started for the first-order Laplacian dynamic based on the graph represented in Figure 2.1.

In Figure 4.1 the magenta lines represent the slow motions of the singular perturbed system (4.4) and the green lines the aggregate model (4.15). The approximation is very precise, thus means that the values of δ and d computed in Section (2.2) are sufficiently small to guarantee accurate results also for systems of the second order.
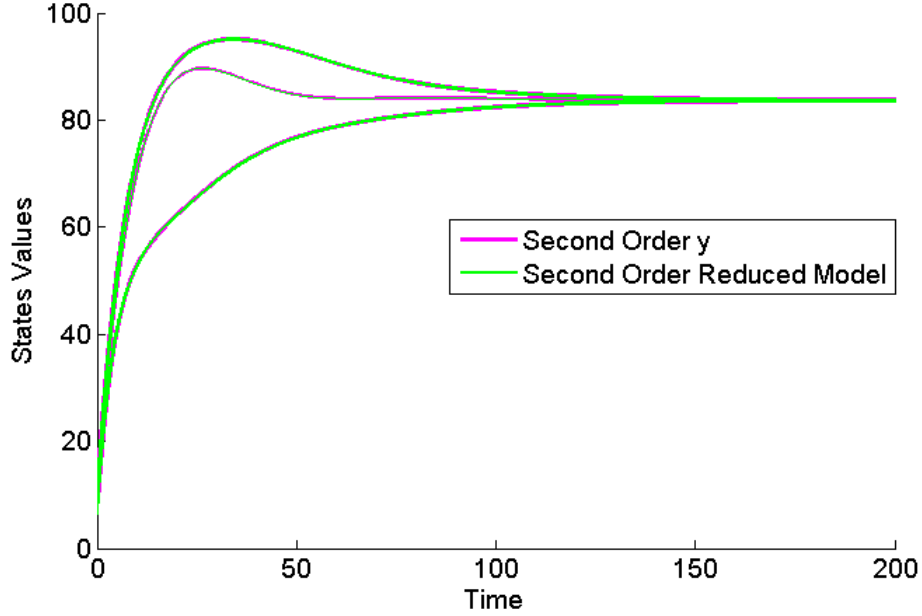
Figure 4.1: Comparison of the evolution on time of the fast motions of system in the singular perturbation form and the boundary layer system

4.2 Aggregate Model

In analogy to the first-order aggregate model (3.2), the system matrix of the second-order aggregate model (4.9) can be rewritten in an insightful way.

We define matrices $\tilde{A}_0, \tilde{L}_a, \tilde{L}_a^I$ with the same definition of (2.21) and (3.1), but considering (4.3) instead than (2.19).

$$\tilde{L}_a \triangleq U^T L^E U,$$
$$\tilde{L}_a^I U^T L^E \tilde{Q} (QM^{-1}L\tilde{Q})^{-1} QM^{-1} L^E U,$$
$$\tilde{L}_{\text{red}} \triangleq (\tilde{L}_a - \tilde{L}_a^I), \tag{4.13}$$
$$\tilde{A}_0 = -M_a^{-1} \tilde{L}_{\text{red}} / (c^I \delta). \tag{4.14}$$

where $H \triangleq U^T L^E M^{-1} Q^T$.

Lemma 4.2.1. (Laplacian properties of the aggregate model II) *The* Reduced Laplacian Matrix *for the second order system $\tilde{L}_{red} \triangleq \tilde{L}_a - \tilde{L}_a^I$ is a generalized Laplacian matrix.*

Proof. The proof can be done adapting Theorem 3.2.2 to $\tilde{L}_a$ and $\tilde{L}_a^I$.

Notice that $\tilde{L}_a = L_a$. It follows that $\tilde{L}_a$ is a Laplacian matrix.

Moreover, $\tilde{L}_a^I$ has the same properties of L_a^I, as we can see defining $H \triangleq U^T L^E M^{-1} Q^T$ and observing:

$$
\begin{aligned}
\tilde{L}_a^I &= H(QM^{-1}Q^T)^{-1}(QM^{-1}LM^{-1}Q^T(QM^{-1}Q^T)^{-1})^{-1}H^T \\
&= H(QM^{-1}Q^T)^{-1}(QM^{-1}Q^T)(QM^{-1}LM^{-1}Q^T)^{-1}H^T \\
&= H(QM^{-1}LM^{-1}Q^T)^{-1}H^T
\end{aligned}
$$

From Lemma 2.3.4 follows $QM^{-1}LM^{-1}Q^T \succ 0$, which implies $\tilde{L}_a^I \succeq 0$. An analysis analogous to that of Theorem 3.2.2 then shows that $\tilde{L}_{\mathrm{red}}$ is a generalized Laplacian matrix. ∎

Finally, the aggregate model (4.15) is rewritten with the original variables $[y^T, \dot{y}^T]^T$ and in time scale t. This yields a nice and compact form to express the aggregate model.

Theorem 4.2.2. (Reformulation of the aggregate model II) *Let $M_a = U^T M U$ and $D_a = U^T M U$ be the aggregate inertia and damping matrices. Then the aggregate model (4.9) reads equivalently as*

$$
M_a \ddot{y} = -D_a \dot{y} - \tilde{L}_{\mathrm{red}} y, \tag{4.15}
$$

where $\tilde{L}_{\mathrm{red}}$ is a generalized Laplacian matrix.

Proof. In analogy to Lemma 3.1.1, we obtain that

Considering (4.14), system (4.9) reads equivalently as

$$
\frac{d}{dt_s}\begin{bmatrix} \bar{y}_s \\ \dot{\bar{y}}_s \end{bmatrix} = \begin{bmatrix} 0 & \frac{I_r}{c^I} \\ -\frac{M_a^{-1}\tilde{L}_{\mathrm{red}}}{c^I \delta} & -\frac{M_a^{-1}D_a}{c^I \sqrt{\delta}} \end{bmatrix} \begin{bmatrix} \bar{y}_s \\ \dot{\bar{y}}_s \end{bmatrix}.
$$

The change of variables $[y_s^T, \dot{y}_s^T]^T = [\bar{y}_s^T, \sqrt{\delta} \cdot \dot{\bar{y}}_s^T]^T$ yields

$$
\frac{d}{dt_s}\begin{bmatrix} y_s \\ \dot{y}_s \end{bmatrix} = \begin{bmatrix} 0 & \frac{I_r}{c^I \sqrt{\delta}} \\ -\frac{M_a^{-1}L_{red}}{c^I \sqrt{\delta}} & -\frac{M_a^{-1}D_a}{c^I \sqrt{\delta}} \end{bmatrix} \begin{bmatrix} y_s \\ \dot{y}_s \end{bmatrix}
$$

Finally, the change of time-scale $t = t_s/(c^I \sqrt{\delta})$ yields

$$\frac{d}{dt} \begin{bmatrix} y_s \\ \dot{y}_s \end{bmatrix} = \begin{bmatrix} 0 & I_r \\ -M_a^{-1} L_{red} & -M_a^{-1} D_a \end{bmatrix} \begin{bmatrix} y_s \\ \dot{y}_s \end{bmatrix}$$

thus is the state space version of system (4.15).

■

5

Simulations

We validated the theoretical developments in this thesis with several test-graphs created on purpose by Matlab routines based on Erdoš-Rényi algorithm and with the RTS 96 power network model shown in Figure 5.1.

5.1   Simulation Results for RTS 96 Power System

The first validating network is the RTS 96, which presents a structure suitable with the characteristics required in Section (2.2), see Figure 5.1.

The RTS 96 consists of $r = 3$ areas and $n = 33$ generators obeying the swing dynamics (2.2), the algebraic load flow is absorbed into the network parameters through Kron reduction Dörfler and Bullo (2011), and the initial angles and frequencies are chosen to be aligned within each area.

For illustrative purposes, we slightly increased the nominal generator damping constants (to reduce large oscillation amplitudes resulting in cluttered plots) and weakened the inter-area line connections by a factor 0.5 in the linearized model (corresponding to a steady state with large inter-area power transfers) resulting in $\delta = 0.3955$.
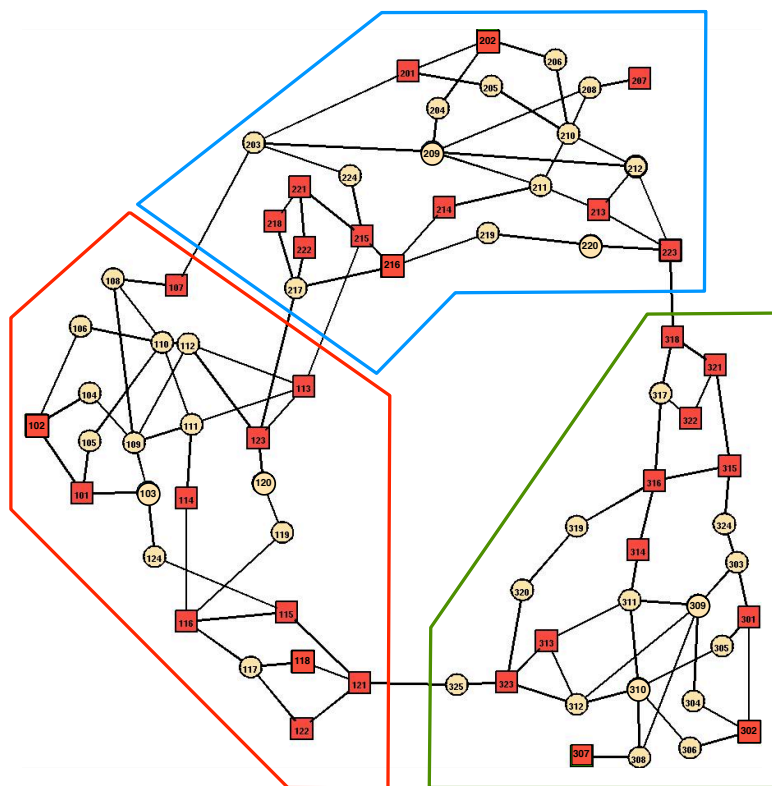
Figure 5.1: Illustration of RTS 96 power network with three areas. Here the square nodes are the generators and the circles the load buses of the network.

All the initial conditions $x(0)$ are clustered, accordingly to the area, in order to have more readable plots but this is noa a necessary condition.

The detailed simulation results are reported in Figure 5.2 and Figure 5.3.

Figure 5.2 shows the evolution on time of system (2.2) and it can be observed that generators within an area swing coherently. This confirm graphically the aggregation theory for nodes strongly connected, as the ones inside one area, and rends the idea why we consider all the nodes in area as a single node.

Figure 5.3 shows the comparison between the aggregate model (4.9) and the singular perturbation model (4.4).

Despite the fact that δ is not infinitesimally small, the reduced model (4.9) accurately approximates the aggregate behavior of the original model (4.4).

Anyway, accordingly to the theory presented, reducing further the weights on the external connections of the graph, and therefore δ, the reduced-order system (4.9) would approximate better the singular perturbed model (4.4).
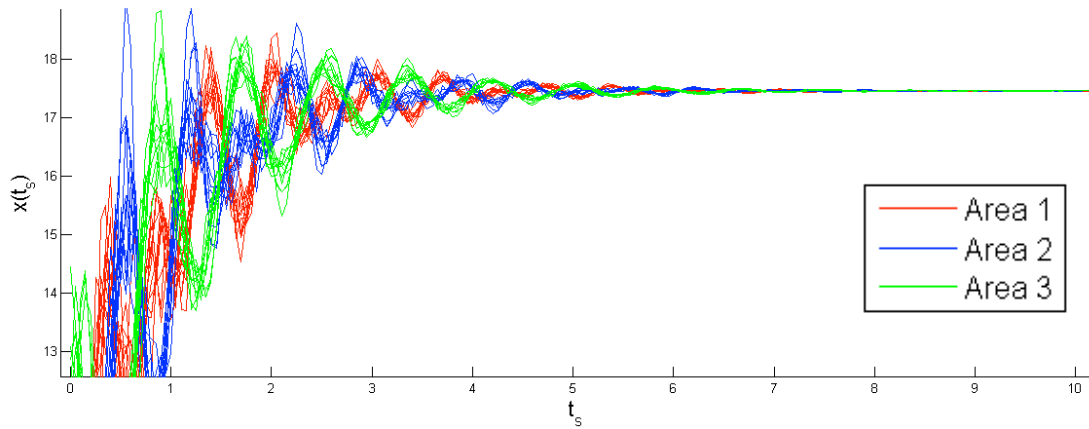
Figure 5.2: Evolution of RTS 96 power network dynamics. All nodes within an area are plotted with the area color indicated in Figure 5.1.
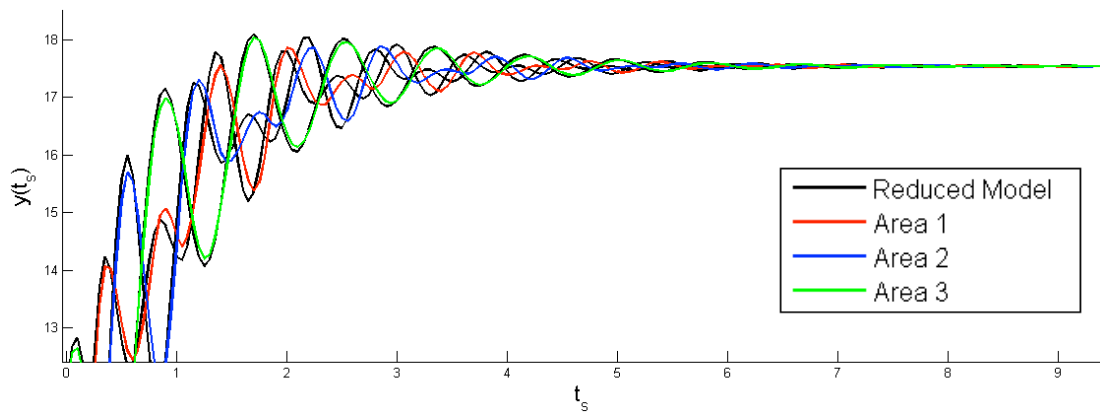
Figure 5.3: Evolution of aggregate variable $y(t_s)$ in original model (4.4) of each area (plotted with the area color indicated in Figure 5.1) and the aggregate variable $\bar{y}(t_s)$ in the reduced model (4.9) (plotted in black).

5.2   Simulation Results for 13-nodes and 3-areas graph

Several random networks generated with routines based on Erdös-Rényi model and respecting the characteristics described in Section (2.2) has been successfully tested, confirming the theory proved in this paper.

The basic process to generate these graphs is:

- generate as many random graph as the number of areas desired

- assign to each node a low connecting probability with nodes of different areas

- guarantee or test that the whole graph is connected

Among all the example graphs tested we present the results with graph in Figure (5.4), which is the same showed in the previous chapters as an illustrative guide of the theoretical results obtained. In this way the analyzis of this graph is complete.
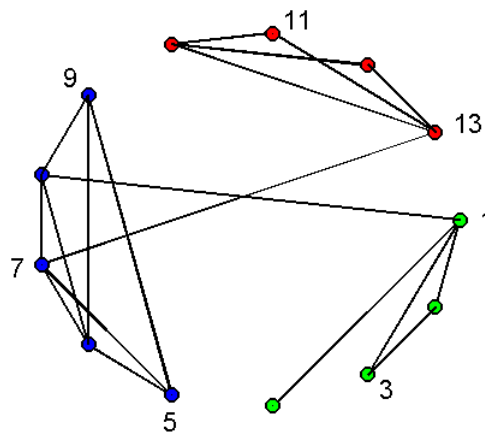
Figure 5.4: 3-Areas and 13-nodes graph.

Figure 5.5 compares the evolutions of the aggregate model (4.15) green lines and the singular perturbed system (4.4) blue lines. The values of the parameters $\delta = 0.1$ and $d = 0.2$ are sufficiently small to guarantee an error between the two systems which is infinitesimal respect the amplitude of the signal, see Figure 5.6. The black lines in Figure 5.5, represent the original system (2.2) which being a second-order system presents oscillations. Notice that the slow motions, by definition, are the center of mass of these oscillations.

In Figure 5.7 the fast motions of (4.4), magenta lines, are compared with the boundary layer system (4.10), blue lines. Again the approximation is very accurate. The error between the two can be seen in Figure 5.8.

Notice that the oscillations of (2.2) in Figure 5.5 last as long as the fast motions in Figure 5.7. This means that the contributions of each single node affect the system just for that short amount of time, after that the nodes within the same area aggregate and behave in the same way.
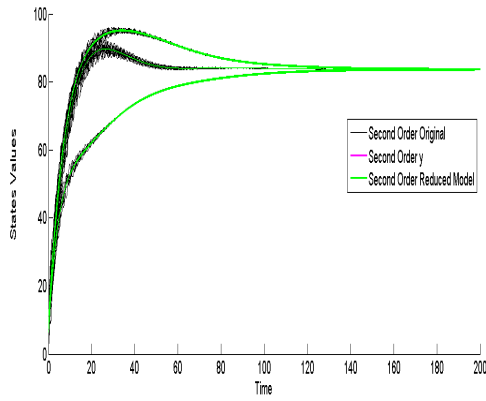
Figure 5.5: Comparison of the evolution on time of the mechanical swing equation, the slow motions of the system in the singular perturbation form and the aggregate model
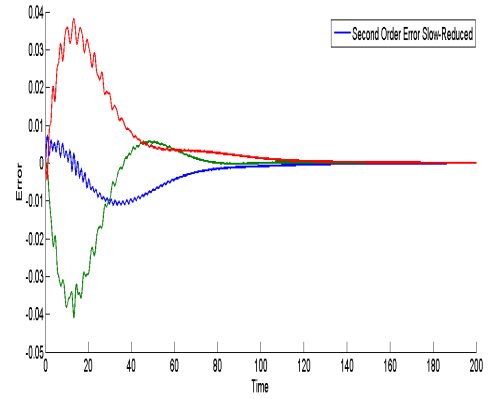
Figure 5.6: Error between the slow motions of the system in the singular perturbation form and of the aggregate model
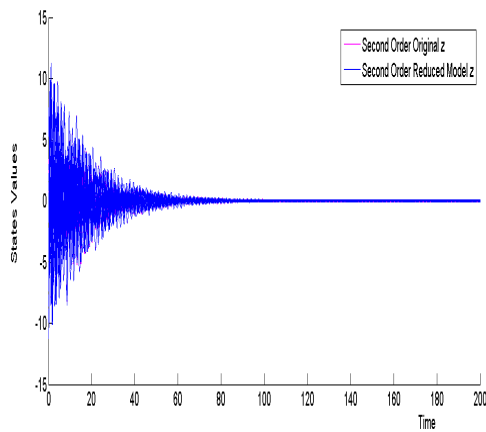
Figure 5.7: Comparison of the evolution on time of the fast motions of system in the singular perturbation form and the boundary layer system
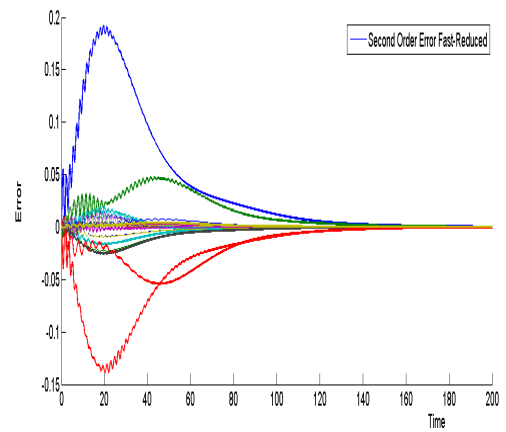
Figure 5.8: Error between the fast motions of the system in the singular perturbation form and the boundary layer system

6

Conclusion

We studied area aggregation and model reduction of first-order consensus and second-order power network dynamics based on slow coherency.

We unified different solutions found in the literature on slow coherency and area aggregation, we relaxed some technical assumptions, and we extended earlier results considering weighted graphs. In particular, for the second-order power network dynamics we provided a complete analyzis without any restriction on the inertia and on the damping of the system.

Finally, we identified the corresponding reduced aggregate models for both first-order and second-order dynamics as generalized Laplacian systems with multiple time constants, aggregate damping and inertia matrices, and possibly adverse interactions. These reduced-order systems retain all the stability properties of Laplacian consensus dynamics and we showed their asymptotic convergence to the same consensus point of the original full-order systems.

Our results provide a solid method to obtain a reduced-order model for the network, an interesting future research direction is to design a control for these models and determine a way to relief it to the original network redistributing the control inputs of each area to each one of its own nodes.

In this direction, we suggest a graph-theoretic analysis relating the Laplacian of

the original model and the generalized Laplacian of the reduced aggregate model. We are deeply convinced that a deeper understanding of the inter-area dynamics serves as a solid foundation for future control design.

References

Biggs N. *Algebraic Graph Theory*. Cambridge University Press, 2 edition, 1994. ISBN 0521458978.

Bıyık E. and Arcak M. Area aggregation and time-scale modeling for sparse nonlinear networks. *Systems & Control Letters*, 57(2):142–149, 2007.

Bullo F., Cortés J., and Martínez S. *Distributed Control of Robotic Networks*. Applied Mathematics Series. Princeton University Press, 2009. ISBN 978-0-691-14195-4.

Chakrabortty A., Chow J. H., and Salazar A. A measurement-based framework for dynamic equivalencing of large power systems using wide-area phasor measurements. *IEEE Transactions on Smart Grid*, 2(1):56–69, 2011.

Chow J. H. *Time-scale modeling of dynamic networks with applications to power systems*. Springer, 1982.

Chow J. H., Allemong J. J., and Kokotović P. V. Singular perturbation analysis of systems with sustained high frequency oscillations. *Automatica*, 14(3):271–279, 1978.

Chow J. H., Cullum J., and Willoughby R. A. A sparsity-based technique for identifying slow-coherent areas in large power systems. *IEEE Transactions on Power Apparatus and Systems*, 103(3):463–473, 1984.

Chow J. H. and Kokotović P. Time scale modeling of sparse dynamic networks. *IEEE Transactions on Automatic Control*, 30(8):714–722, 1985.

Date R. and Chow J. Aggregation properties of linearized two-time-scale power networks. *IEEE Transactions on Circuits and Systems*, 38(7):720–730, 1991.

Dörfler F. and Bullo F. Kron reduction of graphs with applications to electrical networks. *IEEE Transactions on Circuits and Systems I*, November 2011. To appear.

Garin F. and Schenato L. A survey on distributed estimation and control applications using linear consensus algorithms. In **Bemporad A., Heemels M., and Johansson M.**, editors, *Networked Control Systems*, LNCIS, pages 75–107. Springer, 2010.

Khalil H. K. *Nonlinear Systems*. Prentice Hall, 3 edition, 2002. ISBN 0130673897.

Mallada E. and Tang A. Improving damping of power networks: Power scheduling and impedance adaptation. 2011.

Olfati-Saber R., Fax J. A., and Murray R. M. Consensus and cooperation in networked multi-agent systems. *Proceedings of the IEEE*, 95(1):215–233, 2007.

Sauer P. W. and Pai M. A. *Power System Dynamics and Stability*. Prentice Hall, 1998.

Venkatasubramanian V. and Li Y. Analysis of 1996 Western American electric blackouts. In *Bulk Power System Dynamics and Control-VI*, Cortina d'Ampezzo, Italy, 2004.

Zhang F. *The Schur Complement and Its Applications*. Springer, 2005.

Ringraziamenti

I primi doverosi ringraziamenti vanno alla mia numerosa famiglia, ognuno a modo suo ha saputo aiutarmi: mamma e papà con i loro consigli...a volte anche contrastanti tra di loro...mi hanno mostrato i diversi aspetti di ogni problema,e mi hanno supportato in tutto e per tutto!..ma molto di piu hanno sempre reso casa il posto piu accogliente tra i molti visti in mquesti ultimi anni e mi hanno sempre voluto cosÃ\v{} tanto bene da farmi sentire di essere messo prima anche dei loro stessi interessi!grazie...grazie mamma!grazie papà!

Il mio fratellino, che nonostante i suoi tentativi di usurparmi la camera, i suoi tentativi di battermi a braccio di ferro e i suoi tentativi di diventare più alto di me.. mi ha sempre voluto bene in modo smisurato ed è sempre stato pronto a starmi vicino e a farmi sentire che c era. Una persona stupenda.

Le sorellone, la lucertola per i numerosi baci e abbracci che continuamente mi elargiva in segno di profondo affetto e il panda (ormai super dimagrito) per essersi disperata tutte le volte che partivo ..succederanno mai queste cose??..invece, le ringrazio per tutte quelle cose non scritte e non dette ma sentite e vissute, per quella complicità fratello e sorella su cui ho sempre potuto contare, per aver saputo quando era il caso di farsi i fatti loro e quando invece avevo bisogno di loro.

Alla mia dolce morosetta, che più di tutti ne ne ha dovute passare per stare con me in questi anni, il mio vagabondare non le è mai piaciuto ma è riuscita sempre a sopportare in qualche modo e a continuare a starmi vicino aiutandomi a 360 gradi: burocrazia tesi, cucina e pulizie SB, nei miei mille bisogni di ogni giorno e tutto

il sostegno nei momenti di sconforto. Ma ben di più la ringrazio per tutto quello che abbiamo passato insieme e soprattutto per il legame che abbiamo costruito in questo stare insieme, per una storia che non è mai stata semplice ma che mi ha fatto provare emozioni mai provate prima.

Un ringraziamento grande va anche ai miei nonni, i miei zii e zie e tutti i cugini, per l'affetto, la vicinanza e gli scherzi di tutti questi anni!

Just looking at thesis the first thanks should go to Florian, who took care not only of the project itself but also of my understanding and of the development of my own skills. He worked much more than what it was required from his role and he gave me advices that i'll always keep in mind. E a Francesco, non solo un professore che mi ha aiutato ma anche una persona da stimare e di riferimento.

Adesso la carrellata di amici! E per non offendere nessuno, li metterò in ordine alfabetico.

Albi, da anonimo compagno di pallavolo (tra l altro scarso!) è poi diventato l insostituibile compagno di mille esperienze, dalle serate insieme alle skypecall alle fantasticherie su sogni e futuro. Unico.

Albi (Fitz) e Andrea (Wally), le studiate insieme sono state innumerevoli, tanti grandi successi e qualche silurata ogni tanto a cui adesso possiamo riderci sopra!ma molto di più, dei compagni con cui ho avuto un rapporto quasi quotidiano negli ultimi 5 anni.. e nonostante questo, mi hanno sempre accettato per come sono e hanno stretto un legame di amicizia sempre più forte.

Ali, non c e niente da dire...ahahah! Intelligentissima persona con cui da un innumerevole numero di anni ho sempre trovato un feeling di comprensione reciproca che l ha resa unica nella mia vita..un' immancabile amica.

Borghy, Mino e Ricky i primi due i piu fedelissimi seguaci nei miei viaggi, con annessi momenti gloriosi(vedi noiosi pic nic a lisbona, ripetuti passaggi attraverso il buco dell ostello di monaco, imbriagate e cose indicibili..hihi!) il terzo è stato invece il più pacconaro in tutti i viaggi!hihi! Tutti e tre amici storici a cui tengo tantissimo e con cui riesco sempre a stare bene e a godermi i momenti che trascorro loro. Li ringrazio anche per le profonde chiacchierate fatte!

Capu e Gio, appena conosciuti non avrei mai detto sarebbero diventati cosÃň importanti, come invece sono..a quanto pare le distanze geografiche degli ultimi anni non ci hanno allontanato veramente, sono due delle persone che stimo e

rispetto di più!

Cri, che ha sempre organizzato serate e vacanze nella sua casa in campagna e mi ha fatto divertire tantissimo! In tutte le occasioni trascorse, mi ha sempre mostrato la sua amicizia!

Dezu e Matteo..super! Purtroppo, le occasioni di vederci negli ultimi anni non sono state tante, ma ogni volta è stata speciale..tanto divertimento ma anche grandi chiacchierate che mi hanno segnato profondamente!

Diane e lele, non solo coppia che stimo ma anche persone che apprezzo molto per quello che mi hanno mostrato in questi anni.

Dimi, imprevedibile amico con cui ho condiviso tanto e nonostante periodi in cui non siamo riusciti a sentirci molto è sempre riapparso quando avevo bisogno di lui.

Gasta, inummerovali sono i momenti per cui vorrei ringraziarti, dalle chiaccherate nel confessionale alle infinite partite a ping pong alle vacanze omosessuali fatte insieme!indubbiamente tra quelli che hanno segnato di più i miei ultimi 10 anni di vita!

SB friends!! Dome, Filippo, Iris, Marghe e Mattia..quei sei mesi sono stati probabilmente il periodo all estero più bello che io abbia fatto anche grazie a voi! dai bbq sulla spiaggia, alle cene insieme, alle pause caffe e ai pranzi insieme!e grazie a tutti gli altri nostri amici che abbiamo trovato là!!